

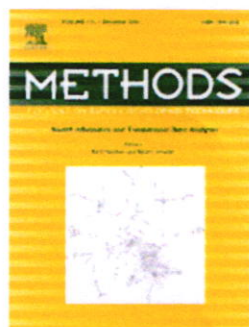


ELSEVIER
ELSEVIER

SEARCH

MENU

Home (<https://www.elsevier.com/>) > Journals (<https://www.elsevier.com/catalog?produc...>)
> Methods (<https://www.journals.elsevier.com:443/methods>)



(<https://www.sciencedirect.com/science/journal/10462023>)

ISSN: 1046-2023

Methods

Editor-in-Chief: Kenneth W. Adolph

(<https://www.journals.elsevier.com:443/methods/editorial-board/kenneth-w-adolph>)

> View Editorial Board (<https://www.journals.elsevier.com:443/methods/editorial-board>)

Supports Open Access (<http://www.elsevier.com/journals/methods/1046-2023/open-access-options>)

View Articles (<https://www.sciencedirect.com/science/journal/10462023>)

Guide for Authors

Abstracting/ Indexing (<http://www.elsevier.com/journals/methods/1046-2023/abstracting-indexing>)

Track Your Paper (<https://authors.elsevier.com/tracking/landingpage/selection.do>)

f (/me (http
(http (//tw thod s://w
://w itter. s/rss) ww.e
ww.f com/ lsevi
aceb elsbi er.co
ook. ome m/Pr
com/dche efere
elsev m) nceC
ierbi entre
ome)
dche
m)

Order Journal

Journal Metrics

> CiteScore: **3.72** ⓘ

Impact Factor: **3.998** ⓘ

5-Year Impact Factor: **3.936** ⓘ

Source Normalized Impact per Paper (SNIP): **0.954** ⓘ

SCImago Journal Rank (SJR): **2.333** ⓘ

Your Research Data

- > Share your research data (<https://www.elsevier.com/authors/author-services/research-data>)
- > Visualize your data (<http://www.elsevier.com/authors/author-services/data-visualization>)

Related Links

- > Author Stats ⓘ
- > Researcher Academy
- > Author Services (<https://www.elsevier.com/authors/author-services>)
- > Try out personalized alert features

Related Publications

Analytical Biochemistry: Methods in the Biological Sciences
(<https://www.elsevier.com/locate/inca/622781>)

MethodsX (<https://www.elsevier.com/locate/inca/731614>)

Methods focuses on rapidly developing **techniques** in the **experimental biological** and **medical sciences**.

Each topical issue, organized by a guest editor who is an expert in the area covered, consists solely of invited quality articles by specialist authors, many of them reviews. Issues are devoted to specific...

[Read more](#)

[Most Downloaded](#) [Recent Articles](#) [Most Cited](#) [Open Access Articles](#)

An introduction to sample preparation and imaging by cryo-electron microscopy for structural biology

Rebecca F. Thompson | Matt Walker | ...

Multiplexed immunohistochemistry, imaging, and quantitation: A review, with an assessment of Tyramide signal amplification, multispectral imaging and multiplex analysis

Edward C. Stack | Chichung Wang | ...

Analysis of Relative Gene Expression Data Using Real-Time Quantitative PCR and the $2^{-\Delta\Delta CT}$ Method

Kenneth J. Livak | Thomas D. Schmittgen

> View All Most Downloaded Articles (<https://www.journals.elsevier.com:443/methods/most-downloaded-articles>)

Most Downloaded Articles



Recent Articles



Most Cited Articles



Recent Open Access Articles



  (/me (<http://twitter.com/elsevier>))

(<http://twitter.com/elsevier>)

Announcements

(<https://www.journals.elsevier.com:443/methods/announcements>)

New guidelines for research data (<https://www.elsevier.com/authors/author-services/research-data/data-guidelines>)

Authors submitting their research article to this journal are encouraged to deposit research data in a relevant data repository and cite and link to this dataset in their article. If this is not possible, authors are encouraged to make a statement explaining why research data cannot be shared. There are several ways you can share your data when you publish with Elsevier, which help you get credit for your work and make your data accessible and discoverable for your peers. Find out more in the Guide for Authors.

Authors submitting their research article to this journal are encouraged to deposit research data in a relevant data repository and cite and link to this dataset in their article. If this is not possible, authors are encouraged to make a statement explaining why research data cannot be shared. There are several ways you can share your data when you publish with Elsevier, which help you get credit for your work and make your data accessible and discoverable for your peers. Find out more in the Guide for Authors.

Authors submitting their research article to this journal are encouraged to deposit research data in a relevant data repository and cite and link to this dataset in their article. If this is not possible, authors are encouraged to make a statement explaining why research data cannot be shared. There are several ways you can share your data when you publish with Elsevier, which help you get credit for your work and make your data accessible and discoverable for your peers. Find out more in the Guide for Authors.

Authors submitting their research article to this journal are encouraged to deposit research data in a relevant data repository and cite and link to this dataset in their article. If this is not possible, authors are encouraged to make a statement explaining why research data cannot be shared. There are several ways you can share your data when you publish with Elsevier, which help you get credit for your work and make your data accessible and discoverable for your peers. Find out more in the Guide for Authors.

Authors submitting their research article to this journal are encouraged to deposit research data in a relevant data repository and cite and link to this dataset in their article. If this is not possible, authors are encouraged to make a statement explaining why research data cannot be shared. There are several ways you can share your data when you publish with Elsevier, which help you get credit for your work and make your data accessible and discoverable for your peers. Find out more in the Guide for Authors.

Authors submitting their research article to this journal are encouraged to deposit research data in a relevant data repository and cite and link to this dataset in their article. If this is not possible, authors are encouraged to make a statement explaining why research data cannot be shared. There are several ways you can share your data when you publish with Elsevier, which help you get credit for your work and make your data accessible and discoverable for your peers. Find out more in the Guide for Authors.

Authors submitting their research article to this journal are encouraged to deposit research data in a relevant data repository and cite and link to this dataset in their article. If this is not possible, authors are encouraged to make a statement explaining why research data cannot be shared. There are several ways you can share your data when you publish with Elsevier, which help you get credit for your work and make your data accessible and discoverable for your peers. Find out more in the Guide for Authors.

More information on Research Data Guidelines (<https://www.elsevier.com/authors/author-services/research-data/data-guidelines>).

[Support](#)
[Training](#)
[Contact Us](#)
[clarivate.com](#)

[Master Journal List](#)
Site

Client

proxystylesheet

Output

Search 

allAreas

Journal Search

Search Terms

Database	Search Type	Title Word
Master Journal List		

Search Term(s): *1046-2023 · The following title(s) matched your request

1-1 of 1 journals



METHODS

Semimonthly

ISSN: 1046-2023

E-ISSN: 1095-9130

ACADEMIC PRESS INC ELSEVIER SCIENCE, 525 B ST, STE 1900, SAN DIEGO, USA, CA, 92101-4495

[Coverage](#)

[Science Citation Index](#)

[Science Citation Index Expanded](#)

[Current Contents - Life Sciences](#)

[BIOSIS Previews](#)

> Author Stats (https://www.mendeley.com/stats/welcome?dgcid=journals_referral_related-links) ⓘ

> Researcher Academy (<https://researcheracademy.elsevier.com>)

> Author Services (<https://www.elsevier.com/authors/author-services>)

> Try out personalized alert features

(https://service.elsevier.com/app/answers/detail/a_id/18726/supporthub/sciencedirect/p/10959?utm_campaign=STMJ_o63818_PA&utm_channel=WEB&utm_source=WEB&dgcid=STMJ_o63818_PA)

Related Publications

Analytical Biochemistry: Methods in the Biological Sciences

(<https://www.elsevier.com/locate/inca/622781>)

MethodsX (<https://www.elsevier.com/locate/inca/731614>)

Methods - Editorial Board

Editor-in-Chief

Kenneth W. Adolph (<https://www.journals.elsevier.com:443/methods/editorial-board/kenneth-w-adolph>)

University of Minnesota, Minneapolis, Minnesota, USA

Editor

Sun Kim (<https://www.journals.elsevier.com:443/methods/editorial-board/sun-kim>)

Seoul National University (SNU), Seoul, The Republic of Korea

Christophe Lavelle

(<https://www.journals.elsevier.com:443/methods/editorial-board/christophe-lavelle>)

Museum National d'Histoire Naturelle, Paris, France



Brian McFarlin (<https://www.journals.elsevier.com:443/methods/editorial->

board/brian-mcfarlin)

University of North Texas, Denton, Texas, USA



Michelle Peckham (<https://www.journals.elsevier.com:443/methods/editorial-board/michelle-peckham>)

University of Leeds, Leeds, England, UK

Nils Walter (<https://www.journals.elsevier.com:443/methods/editorial-board/nils-walter>)

University of Michigan, Ann Arbor, Michigan, USA

Editorial Board

Karen Adelman

Harvard Medical School, Boston, USA

Jurg Bahler

University College London (UCL), London, UK

Vytas Bankaitis

University of North Carolina at Chapel Hill School of Medicine, Chapel Hill, North Carolina, USA

Toni Cathomen

Universitätsklinikum Freiburg, Freiburg, Germany

Jonathan Chaires

University of Louisville, Louisville, Kentucky, USA

David Corey

University of Texas Southwestern Medical Center, Dallas, Texas, USA

Nancy Cox

University of Chicago, Chicago, Illinois, USA

Jack E. Dixon

University of California at San Diego (UCSD), La Jolla, California, USA



SEARCH



MENU

Erica A. Golemis

Fox Chase Cancer Center, Philadelphia, Pennsylvania, USA

(<https://www.elsevier.com>)

Allan Jacobson

University of Massachusetts Medical School, Worcester, Massachusetts, USA

Ulf Landegren

Uppsala Universitet, Uppsala, Sweden

David M.J. Lilley

University of Dundee, Dundee, Scotland, UK

James Manley

Columbia University, New York, New York, USA

Lynne Maquat

University of Rochester, Rochester, New York, USA

Joachim Messing

Rutgers University, Piscataway, New Jersey, USA

Tom Misteli

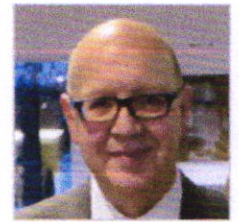
(<https://www.journals.elsevier.com:443/methods/editorial-board/tom-misteli>)

National Cancer Institute (NCI), Bethesda, Maryland, USA



Stephen Neidle (<https://www.journals.elsevier.com:443/methods/editorial-board/stephen-neidle>)

University College London (UCL), London, UK



Michael Pfaffl (<https://www.journals.elsevier.com:443/methods/editorial-board/michael-pfaffl>)

Technische Universität München, Freising-Weihenstephan, Germany

Cenk Sahinalp

Simon Fraser University, Burnaby, British Columbia, Canada

Thomas Schmittgen

University of Florida Health Science Center, Gainesville, Florida, USA

Marc H.V. Van Regenmortel

(<https://www.journals.elsevier.com:443/methods/editorial-board/marc-hv-van-regenmortel>)

Université de Strasbourg, Illkirch, France

Johannes Walter

Harvard Medical School, Boston, Massachusetts, USA

Wei Wang

University of California at San Diego (UCSD), La Jolla, California, USA

Limsoon Wong

National University of Singapore, Singapore, Singapore

Jerry Workman

Stowers Institute for Medical Research, Kansas City, Missouri, USA

Methods

Readers

[View Articles \(https://www.sciencedirect.com/science/journal/10462023\)](https://www.sciencedirect.com/science/journal/10462023)
[Volume/ Issue Alert \(https://www.sciencedirect.com/user/alerts\)](https://www.sciencedirect.com/user/alerts)
[Personalized Recommendations \(https://www.sciencedirect.com/user/register?utm_campaign=sd_recommender_ELSJLS&utm_channel=elseco&dgcid=sd_recommender_ELSJLS\)](https://www.sciencedirect.com/user/register?utm_campaign=sd_recommender_ELSJLS&utm_channel=elseco&dgcid=sd_recommender_ELSJLS)

[Authors \(http://www.elsevier.com/authors/home\)](http://www.elsevier.com/authors/home)
[Author Information Pack \(http://www.elsevier.com/journals/methods/1046-2023?generatepdf=true\)](http://www.elsevier.com/journals/methods/1046-2023?generatepdf=true)
[Track Your Paper \(http://help.elsevier.com/app/answers/detail/a_id/89/p/8045/\)](http://help.elsevier.com/app/answers/detail/a_id/89/p/8045/)
[Early Career Resources \(http://www.elsevier.com/early-career-researchers/training-and-workshops\)](http://www.elsevier.com/early-career-researchers/training-and-workshops)
[Rights and Permissions \(https://www.elsevier.com/about/policies/copyright/permissions\)](https://www.elsevier.com/about/policies/copyright/permissions)
[Webshop \(http://webshop.elsevier.com/\)](http://webshop.elsevier.com/)
[Support Center \(https://service.elsevier.com/app/home/supporthub/publishing/#authors\)](https://service.elsevier.com/app/home/supporthub/publishing/#authors)

[Librarians \(https://www.elsevier.com/librarians\)](https://www.elsevier.com/librarians)
[Ordering Information and Dispatch Dates \(http://www.elsevier.com/journals/methods/1046-2023/order-journal\)](http://www.elsevier.com/journals/methods/1046-2023/order-journal)
[Abstracting/ Indexing \(http://www.elsevier.com/journals/methods/1046-2023/abstracting-indexing\)](http://www.elsevier.com/journals/methods/1046-2023/abstracting-indexing)

[Editors \(http://www.elsevier.com/editors/home\)](http://www.elsevier.com/editors/home)
[Publishing Ethics Resource Kit \(http://www.elsevier.com/editors/perk\)](http://www.elsevier.com/editors/perk)
[Guest Editors \(http://www.elsevier.com/editors/guest-editors\)](http://www.elsevier.com/editors/guest-editors)
[Support Center \(https://service.elsevier.com/app/home/supporthub/publishing/#editors\)](https://service.elsevier.com/app/home/supporthub/publishing/#editors)

[Reviewers \(http://www.elsevier.com/reviewers/home\)](http://www.elsevier.com/reviewers/home)
[Reviewer Guidelines \(http://www.elsevier.com/reviewersguidelines\)](http://www.elsevier.com/reviewersguidelines)
[Log in as Reviewer \(https://www.evise.com/profile/api/navigate/METHODS\)](https://www.evise.com/profile/api/navigate/METHODS)
[Reviewer Recognition \(https://www.elsevier.com/reviewers/becoming-a-reviewer-how-and-why#recognizing\)](https://www.elsevier.com/reviewers/becoming-a-reviewer-how-and-why#recognizing)
[Support Center \(https://service.elsevier.com/app/home/supporthub/publishing/#reviewers\)](https://service.elsevier.com/app/home/supporthub/publishing/#reviewers)

[Advertisers Media Information \(https://www.elsevier.com/advertisers\)](https://www.elsevier.com/advertisers)

[Societies \(http://www.elsevier.com/societies/home\)](http://www.elsevier.com/societies/home)



[\(https://www.elsevier.com\)](https://www.elsevier.com)

ELSEVIER

Copyright © 2019 Elsevier B.V.

[Careers \(https://www.elsevier.com/careers/careers-with-us\)](https://www.elsevier.com/careers/careers-with-us) - [Terms and Conditions](#)

[\(https://www.elsevier.com/legal/elsevier-website-terms-and-conditions\)](https://www.elsevier.com/legal/elsevier-website-terms-and-conditions) - [Privacy Policy](#)

[\(https://www.elsevier.com/legal/privacy-policy\)](https://www.elsevier.com/legal/privacy-policy)

Cookies are used by this site. To decline or learn more, visit our [Cookies \(/Cookies\)](#) page.



ELSEVIER

(<https://www.elsevier.com>) & RELX Group™ (<http://www.reedelsevier.com/>)



(<https://www.mendeley.com/groups/>) & RELX Group™ (<http://www.reedelsevier.com/>)

(<https://twitter.com/Elsevier>) (<https://www.facebook.com/Elsevier>) (<https://www.linkedin.com/company/elsevier>)
com/Elsevier. kedin.c
evierCo com/Elsevier/co
nnect) evierCo mpany/
nnect) reed-
elsevier)

" "



Methods

SUPPORTS OPEN ACCESS

[Articles in press](#)

[Latest issue](#)

[Special issues](#)

[All issues](#)

[Sign in to set up alerts](#)

Affinity-Based Separation Methods for the Study of Biological Interactions

Edited by David S. Hage

Volume 146, Pages 1-126 (15 August 2018)

[← Previous vol/issue](#)

[Next vol/issue >](#)



Show all article previews



Download PDFs



Export

● Full text access

Editorial Board

Page ii

 [Download PDF](#)

Editorial ○ No access

Affinity-Based Separation Methods for the Study of Biological Interactions

David S. Hage

Pages 1-2

 [Purchase PDF](#)

Review article ○ Abstract only

Analysis of solute-protein interactions and solute-solute competition by zonal elution affinity chromatography

Pingyang Tao, Saumen Poddar, Zuchen Sun, David S. Hage, Jianzhong Chen

Pages 3-11

 [Purchase PDF](#) [Article preview](#) 

Review article ○ Abstract only

Affinity-based separation methods for the study of biological interactions: The case of peroxisome proliferator-activated receptors in drug discovery

Caterina Temporini, Gloria Brusotti, Giorgio Pochetti, Gabriella Massolini, Enrica Calleri

Pages 12-25

 [Purchase PDF](#) [Article preview](#) 

Review article ○ Abstract only

Fragment screening for drug leads by weak affinity chromatography (WAC-MS)

Sten Ohlson, Minh-Dao Duong-Thi

Pages 26-38

 [Purchase PDF](#) [Article preview](#) 













Research article ○ Abstract only

Peak decay analysis and biointeraction studies of immunoglobulin binding and dissociation on protein G affinity microcolumns

Jeanethe A. Anguizola, Erika L. Pfaunmiller, Mitchell L. Milanuk, David S. Hage

Pages 39-45

 [Purchase PDF](#) [Article preview](#) 

- Research article Abstract only
Characterization of solution-phase drug-protein interactions by ultrafast affinity extraction
Sandya R. Beeram, Xiwei Zheng, Kyungah Suh, David S. Hage
Pages 46-57
 [Purchase PDF](#) [Article preview](#) 
- Research article Abstract only
Thread- paper, and fabric enzyme-linked immunosorbent assays (ELISA)
Ariana Gonzalez, Michelle Gaines, Laura Y. Gallegos, Ricardo Guevara, Frank A. Gomez
Pages 58-65
 [Purchase PDF](#) [Article preview](#) 
- Review article Abstract only
Studies of antibody-antigen interactions by capillary electrophoresis: A review
Annette C. Moser, Sidney Trenhaile, Kati Frankenberg
Pages 66-75
 [Purchase PDF](#) [Article preview](#) 
- Review article Abstract only
Affinity capillary electrophoresis for studying interactions in life sciences
Mais Olabi, Matthias Stein, Hermann Wätzig
Pages 76-92
 [Purchase PDF](#) [Article preview](#) 
- Review article *Open access*
Advances in enzyme substrate analysis with capillary electrophoresis
Srikanth Gattu, Cassandra L. Crihfield, Grace Lu, Lloyd Bwanali, ... Lisa A. Holland
Pages 93-106
 [Download PDF](#) [Article preview](#) 
- Review article Abstract only
Thermophoresis for characterizing biomolecular interaction
Mufarreh Asmari, Ratih Ratih, Hassan A. Alhazmi, Sami El Deeb
Pages 107-119
 [Purchase PDF](#) [Article preview](#) 

Research article Abstract only

Temperature controlled ionic liquid aqueous two phase system combined with affinity capillary electrophoresis for rapid and precise pharmaceutical-protein binding measurements

Deia Abd El-Hady, Hassan M. Albishri

Pages 120-125

 [Purchase PDF](#) [Article preview](#) 

ISSN: 1046-2023

Copyright © 2019 Elsevier Inc. All rights reserved

ELSEVIER [About ScienceDirect](#) [Remote access](#) [Shopping cart](#) [Contact and support](#) [Terms and conditions](#)
[Privacy policy](#)

We use cookies to help provide and enhance our service and tailor content and ads. By continuing you agree to the [use of cookies](#).

Copyright © 2019 Elsevier B.V. or its licensors or contributors. ScienceDirect® is a registered trademark of Elsevier B.V.

 **RELX Group™**



Thermophoresis for characterizing biomolecular interaction

Mufarreh Asmari^a, Ratih Ratih^a, Hassan A. Alhazmi^b, Sami El Deeb^{a,*}

^a Institute of Medicinal and Pharmaceutical Chemistry, TU Braunschweig, Beethovenstrasse 55, 38106 Braunschweig, Germany

^b College of Pharmacy, Jazan University, P.O. Box 114, 45142 Jazan, Saudi Arabia



ARTICLE INFO

Article history:

Received 30 November 2017
Received in revised form 6 February 2018
Accepted 9 February 2018
Available online 10 February 2018

Keywords:

Microscale thermophoresis
Binding interactions
Binding constant
Hill equation

ABSTRACT

The study of biomolecular interactions is crucial to get more insight into the biological system. The interactions of protein-protein, protein-nucleic acids, protein-sugars, nucleic acid-nucleic acids and protein-small molecules are supporting therapeutics and technological developments. Recently, the development in a large number of analytical techniques for characterizing biomolecular interactions reflect the promising research investments in this field.

In this review, microscale thermophoresis technology (MST) is presented as an analytical technique for characterizing biomolecular interactions. Recent years have seen much progress and several applications established. MST is a powerful technique in quantitation of binding events based on the movement of molecules in microscopic temperature gradient. Simplicity, free solutions analysis, low sample volume, short analysis time, and immobilization free are the MST advantages over other competitive techniques. A wide range of studies in biomolecular interactions have been successfully carried out using MST, which tend to the versatility of the technique to use in screening binding events in order to save time, cost and obtained high data quality.

© 2018 Elsevier Inc. All rights reserved.

Contents

1. Introduction	108
2. Thermophoresis	108
2.1. Overview	108
2.2. Microscale thermophoresis	108
2.2.1. Theoretical background of MST	108
2.2.2. MST instruments	109
2.2.3. MST experimental setup and optimizations	110
2.2.4. MST data analysis	111
3. Applications	111
3.1. MST of protein interactions	111
3.1.1. Protein-protein interactions	111
3.1.2. Protein-small molecule interaction	113
3.2. MST of nucleic acids interactions	113
3.3. MST nucleic acids aptamer interactions	115
3.4. MST of miscellaneous applications	116
4. Conclusion	117
Acknowledgment	117
References	117

* Corresponding author.

E-mail address: s.eldeeb@tu-bs.de (S. El Deeb).

1. Introduction

Biomolecular interactions are fundamental nowadays to provide a good understanding towards most of bioprocesses in living systems. Thus, characterization of protein-protein, protein-nucleic acids, protein-sugars, nucleic acid-nucleic acids and protein-small molecules is important and crucial in the life sciences and provides deep insight into the biological outcomes that may help in disease diagnosis, prognosis and therapeutics as well improve the quality of the life [1–3]. Various analytical techniques that have been used to characterize biomolecular interactions. Some of these techniques include affinity-based separation techniques, which represent the major domain of affinity chromatography, [4–6] and affinity capillary electrophoresis [7–9] as well as equilibrium dialysis, which is still interesting and widely used especially in drug-protein interaction studies [10–12]. On the other hand, biochemical and biophysical techniques are attractive and developed dramatically to be the first choice in studying biomolecular interactions. Examples include spectroscopic techniques [13–18], surface plasma resonance (SPR) [19–21], isothermal titration calorimetry (ITC) [22–24] and microscale thermophoresis (MST) [25–27]. This review will discuss thermophoresis in the characterization of biomolecular interactions. The technique is gaining popularity in recent years as a powerful technique in the characterization of biomolecular interaction. In this paper, theory, fundamentals, technical and practical considerations are discussed in detail. Different applications that use microscale thermophoresis as a selected analytical technique in biomolecular interaction studies are followed by a discussion to such literature examples.

2. Thermophoresis

2.1. Overview

Thermophoresis, also known as thermal diffusion or Soret effect, is a physical phenomenon corresponding to the direct motion of molecules induced by a temperature gradient, typically from the hot zone to cold zone. Thermophoresis was discovered by Ludwig in the 19th century and has since been widely applied in inorganic chemistry and polymer separations [28]. Dieter Braun and Albert Libchaber reported for the first time the thermophoretic diffusion of DNA and quantified thermal diffusion constant using fluorescence dyes and laser heating; thus, a new approach has been introduced to study thermophoresis for biomolecules [29]. Robert Piazza and co-workers presented a case study of protein solutions and provided theoretical explanations to thermal diffusion of lysozyme protein [30,31]. Philip Reineck and co-workers investigated thermophoresis of single-strand DNA in microscopic scale rectangular capillary with a 50- μm cross-section and pointed out that use of capillary is reliable as a microfluid environment to investigate optically thermophoresis in solution [32]. Thereafter, thermophoresis in microscale measurements was introduced in the realm of binding studies. Furthermore, MST has been developed in order to address obstacles such as labeling specificity and protein stability. MST label-free system was introduced by Susanne A. I. Seidel and coworkers to study protein-ligand interaction depending on intrinsic tryptophan residues in protein [33].

2.2. Microscale thermophoresis

Microscale thermophoresis (MST) is defined as a method of monitoring the movement of fluorescent molecules through a microscopic temperature gradient. This technique depends on thermophoresis principle of detecting optical fluorescence proper-

ties to analyses the binding affinity of different molecules. MST displays molecular thermal diffusion in few microliters of sample solution [34]. Thus, MST has several advantages over other fluorescence-based analytical techniques, such as simplicity, low sample volume, label-free options, and detecting changes in hydration shell and charges of biomolecules as well as size changes through the binding events [35]. Additionally, MST overcomes some technical obstacles for non-fluorescent techniques; MST offers the immobilization-free system in comparison to SPR, which needs surface artifact. ITC consumed high volumes of sample in comparison to MST which consumed μl -volume of sample regardless of time, system complications and low throughput which gives significant preference for MST. Therefore, MST monitors molecular thermophoresis, which relies on numerous molecular properties and thus provides versatility in applicability and system flexibility [26,34–36].

2.2.1. Theoretical background of MST

Through infrared (IR) laser beam with emission wavelength 1480 nm (Fig. 1A), the local heating of aqueous solution in diameter of $\sim 50\ \mu\text{m}$ and temperature difference $\Delta T \sim 2\text{--}6\ \text{K}$ will generate molecular flow (j) which is directly proportional to temperature gradient with proportionality constant D_T . In steady state, thermophoretic flow opposed by mass diffusion and both effects being balanced, which describe as:

$$j = -cD_T \text{ grad } T$$

$$j = -D \text{ grad } c$$

j : molecular flow; c : molecular concentration; D_T : Thermal diffusion coefficient; T : temperature; D : diffusion coefficient. The D/DT ratio is defined as a Soret coefficient (S_T):

$$S_T = \frac{D}{D_T}$$

S_T describes the concentration ratio under steady-state conditions and given by:

$$S_T : \frac{C_{hot}}{C_{cold}} = \exp(-S_T \Delta T)$$

where C_{hot} is the concentration of molecules at the hot zone and C_{cold} is the concentration of molecules at the cold zone. S_T is Soret coefficient, which is affected by the factors described in the following equation:

$$S_T = \frac{A}{kT} \left(-\Delta S_{hyd}(T) + \frac{\beta \sigma_{eff}^2}{4\epsilon \epsilon_0 T} \times \lambda_{DH} \right)$$

where A is the surface area of the molecules, k is Boltzmann constant, T is temperature of system, σ_{eff} is the effective charge, ΔS_{hyd} is the hydration shell effect, λ_{DH} is the Debye-Hückel screening length, ϵ is the dielectric constant, and β is temperature derivative of ϵ . Therefore, since the conformational changes are dealing with the biomolecules such as effective charges, hydration entropy or molecular surface area provide information for binding affinity.

In principle, MST signal that obtained involves numerous subsequent processes. Initially, MST records fluorescence in the focal IR-laser zone at ambient temperature without laser heating, which is called initial state (Fig. 1B-I). Next, IR-laser turns on heating specific focal zones in the sample solution and leads to changes in fluorescence intensity known as T-jump (Fig. 1B-II). After T-jump, thermophoretic movements of the molecules start and fluorescence intensity will decrease till it reaches the steady state, depending on molecular depletion out of the heated zone according to the typical thermophoresis, described as the movement of molecules from hot to cold zone (Fig. 1B-III). Thereafter, IR-laser

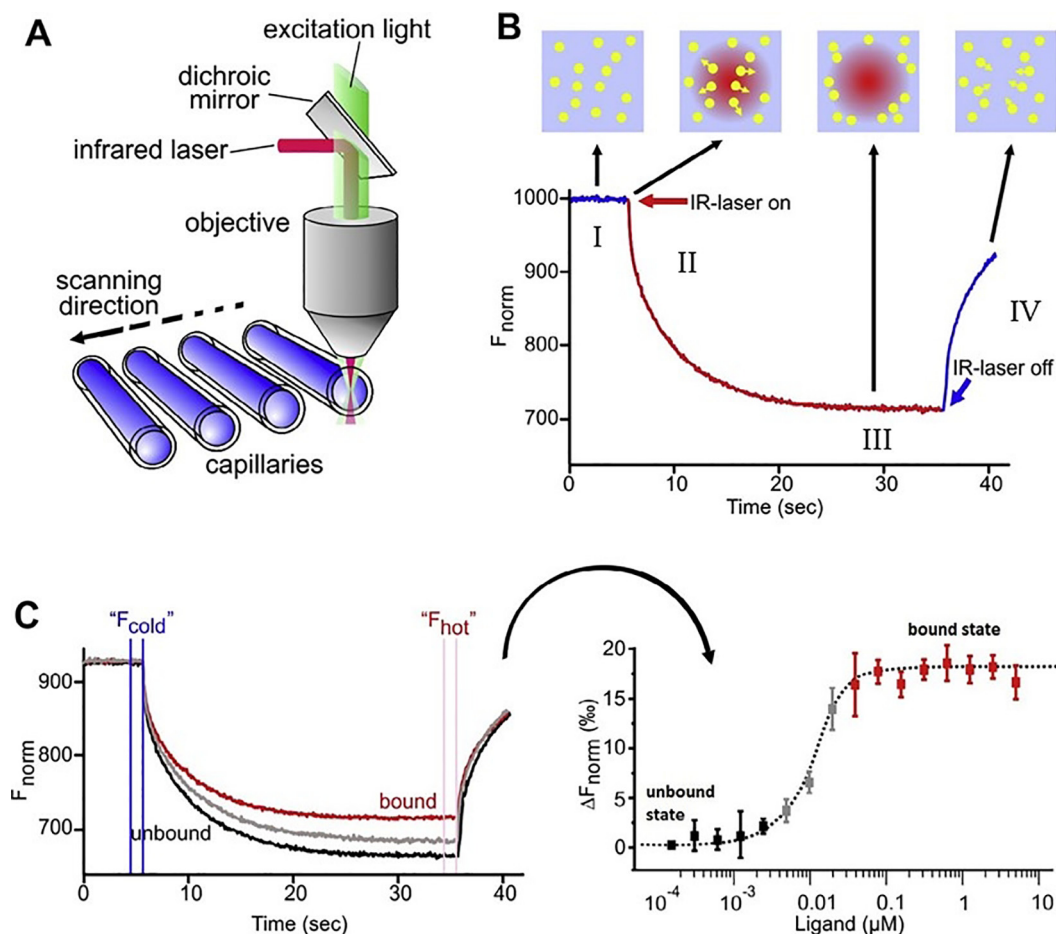


Fig. 1. A) Schematic setup of MST instrument. B) Thermophoresis signal. C) Thermophoretic signals for bound/unbound molecules (left), Binding curve (right). (Adapted with permission from Ref. [28]).

switches off to induce mass diffusion of molecules, depending on concentration gradient, called back-diffusion state (Fig. 1B-IV). The total time for each MST signal takes ~ 35 s. Herein, binding quantifications is taking place by analyzing the change in fluorescence intensity, which is estimated as relative fluorescence (normalized fluorescence), according to the following equation:

$$F_{norm} = F_{hot}/F_{cold}$$

where, F_{norm} : normalized fluorescence; F_{hot} : fluorescence in heated zone; F_{cold} : fluorescence at initial state or in cooling state. The differences in F_{norm} of the bound and unbound state (depend on the concentration of titrated partner) allow to estimate fraction bound (FB) according to the following equation:

$$F_{norm} = (1 - FB)F_{norm}(unbound) + (FB)F_{norm}(bound)$$

Thus, F_{norm} is used to quantify the concentration of fluorescent molecules, which are temperature dependent and governed by the flowing equation:

$$F_{norm} = F_{hot}/F_{cold} = 1 + \left(\frac{\delta F}{\delta T} - S_T \right) \Delta T = \frac{C_{hot}}{C_{cold}} + \frac{\delta F}{\delta T} \Delta T$$

2.2.2. MST instruments

MST instrument consists of optic, which allows the visible light to trigger fluorescence excitation and emission in specific μm -zone for the sample. Infrared IR-laser with a wavelength 1480 nm is reflected using a dichroic mirror to couple into the same path of visible light (Fig. 1A). This well-designed setup with IR radiations

focused on the spot that the fluorescence is measured to exhibit precise observation for sample thermophoresis. To our knowledge, there is one brand for manufacturing of MST instruments. Whereas Nano-temper technologies GmbH (Munich, Germany) offered different types of MST instruments they all possess the same principle but differentiates in detection capabilities. The Monolith NT.115 MST instrument possesses different types of LED-filter: blue (excitation 460–480 nm, emission 515–530 nm), green (excitation 515–525 nm, emission 560–585 nm), red (excitation 605–645 nm, emission 680–685). However, there are different models of Monolith NT.115 MST instruments depending on the range of detection. These types of instrument are used to quantify biomolecular interactions via detection of fluorescent dyes or fluorescent fusion protein. The Monolith NT.115 Label-Free MST instrument has an excitation wavelength of 280 nm and an emission wavelength of 360 nm as well as the detection of visible light with a wavelength range of 480–720 nm, which allow detecting of intrinsic molecular fluorescence in this range without the need to label procedures. In this regard, proteins with high tryptophan contents are more suitable for investigation using Monolith NT.115 Label-Free MST instrument. On the other hand, the Monolith NT.115^{Pico} MST instrument is designed for high-affinity interactions with a sub-Nanomolar scale that enable to detect any red emitted fluorophores in low-picomolar concentrations. Furthermore, to minimize human errors and provide better control of analysis, the automation of MST system has been developed as Monolith NT. automated MST instrument. The MST instrument has a capacity of up to 16 samples that can be loaded in each run and the sample

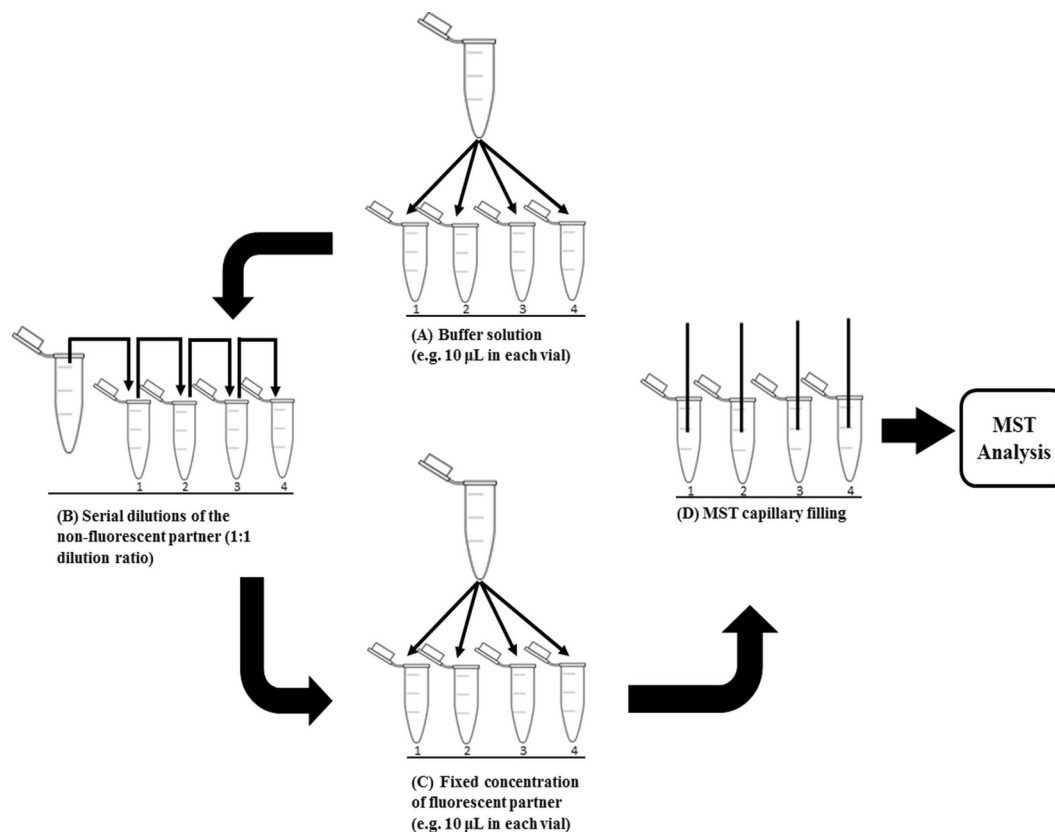


Fig. 2. General scheme for sample preparation steps.

volume of 4 µL. Capillaries are made of pure glass for standard use; coated capillaries can be used for sticky samples to avoid sample adsorption to the capillary wall.

2.2.3. MST experimental setup and optimizations

The good experimental design is the key to work. MST like all analytical techniques, needs to perform experimental setup and optimization of experimental conditions as shown in the general scheme which explains series of preparation steps for MST experiment (Fig. 2). Hence, concentration range, labeling procedures, solvent, proper select of the capillary, capillary filling, LED set and Temperature set should be conducted carefully to achieve good MST measurements.

2.2.3.1. Labeling procedures. MST detection as mentioned before depends on measuring the fluorescence intensity of labeled partner or intrinsic fluorophores in label-free MST system. Therefore, labeling procedure is critical for MST experiments to provide highly sensitive measurements of labeled molecules. Typically, the labeling process is conducted through linking of the specific functional group in dye to crosslinker reactive group. For example, using N-hydroxysuccinimide esters known as "NHS-ester" as linkers to react with a primary amine in targeted protein as well Malimide dyes are used to bind with sulfhydryl groups present in reduced cysteine. However, these types of labeling need washing-up steps before the MST measurements to remove unreacted dye molecules. Alternatively, recombinant proteins which contain fluorescence protein such as green fluorescence protein can be used to fused with specific peptide sequence. Generally, in all fluorescence ligand-based binding assays including MST, the labeling process is a significant pitfall and may alter the ligand properties, regardless of time consumed, multi-cleaning steps and

difficult optimization for some biomolecules. In addition, MST in principle is not affected by fluorescent position or fluorescence levels when compared with other competitive techniques, whereas thermophoresis responds to minor changes inside the system such as charges, hydration shells as well as molecular size [26,33,37].

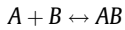
2.2.3.2. Solvent and concentration range considerations. It is known that MST technique is compatible with all buffering systems, without restrictions. However, the buffer may play a critical role in protein aggregations. Yexuan Mao et al. [27] reported the effect of solvents on the aggregation of human islet amyloid polypeptides [11–20]. They found different behaviors of the peptides aggregation under different buffering systems. On the other hand, MST instruments have different capabilities for fluorescence detection in wide concentration ranges; however, in low picomolar concentrations, the quantification of molecular interactions is difficult although it was detected. Therefore, use of Monolith NT.115^{pico} is necessary for accurate quantitative measurements [38].

2.2.3.3. Capillary. In MST technique, the samples were loaded in capillaries with well-defined capacity, outer and inner diameters, because all of these factors affect MST measurements. In each experiment, 16 samples can be loaded into capillaries tray. The sample loading occurs through capillary forces. Therefore, capillary scanning test is critical prior to each measurement to optimize the MST experiment and avoid any handling errors, sample adsorption or fluorescence quenching/enhancement by ligand. To avoid sample adsorption, different types of coated capillaries with hydrophobic/hydrophilic polymers can be used as alternatives to standard glass capillaries or add detergent to the buffer system.

2.2.3.4. LED and temperature set. Manipulation of excitation light power and temperature is enabled in an MST instrument, to obtain a proper fluorescence intensity and thermophoresis. The excitation light power called “LED power” could be set with different power intensity to obtain fluorescence intensity between 200 and 1500 counts, which is suitable signal detections. Laser intensity called “MST power” could be manipulated to induce optimal thermophoresis and raise local temperature between 2 °C and 6 °C.

2.2.4. MST data analysis

Currently, MST data fit in two different binding models which solved by available Nanotemper software. First model, is K_d model which is driven from law of mass action:



A: binding partner A; B: binding partner B; AB: complex

The equilibrium dissociation constant K_d as:

$$K_d = \frac{[A]_{free} - [B]_{free}}{[AB]}$$

Whereas, free concentrations of each partner are not known. Total concentrations are used according to the following formula:

$$[A] = [A]_{free} + [AB] \text{ and } [B] = [B]_{free} + [AB]$$

$[A]_{free}$: free concentration of partner A; $[B]_{free}$: free concentration of partner B; $[AB]$: bound complex concentration.

Hence, K_d is calculated as follow:

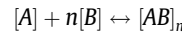
$$K_d = \frac{([A] - [AB])([B] - [AB])}{[AB]}$$

Then, fraction bound FB is calculated as a total concentration of A and B and correlated with K_d parameter as follows:

$$FB = \frac{[A] + [B] + K_d - \sqrt{([A] + [B] + K_d)^2 - 4[AB]}}{2[B]}$$

Where, FB represents linearity with normalized fluorescence form MST measurements. The binding curve is obtained by plotting normalized fluorescence F_{norm} on y-axis against total concentration

of titrated partner and dissociation constant K_d can be determined easily. The aforementioned model is fitted with obtained data if the binding ratio is 1:1 stoichiometry. In more complicated binding ration, Hill equation is the second model to estimate EC50 value, which is defined as a half maximum concentration of titrated binding partner. EC50 is not a physical constant and provide information about the cooperativity of binding events in multivalent interactions. EC50 from Hill equation can be represented as follow:



Where, n is Hill coefficient and FB can have calculated as follow:

$$FB = \frac{1}{1 + (EC50/B)^n}$$

B: provided concentration of titrated partner.

3. Applications

3.1. MST of protein interactions

Protein interactions exhibit important roles in many cellular processes, such as cell regulation and transportation, and to induce of many cellular functions. Therefore, *in vitro* approaches to measuring biomolecular interactions have a great effect to technological applications such as antigen–antibodies affinity, protein characterization, stabilities and drug discoveries. Herein, we provide an overview using of MST of protein interactions for different applications.

3.1.1. Protein-protein interactions

The applications of MST in protein–protein interactions vary and are growing. For example, Wienken et al. [28] introduced MST for the first time in the characterization of immunoaffinity for targeted proteins. The first approach described interaction between human interferon-gamma (hIFN- γ) and IFN- γ antibodies whereas; the second approach determined affinity between green fluorescent protein (GFP) and small antibody fragment, known as GFP-binding protein (GBP). The dissociation constants were

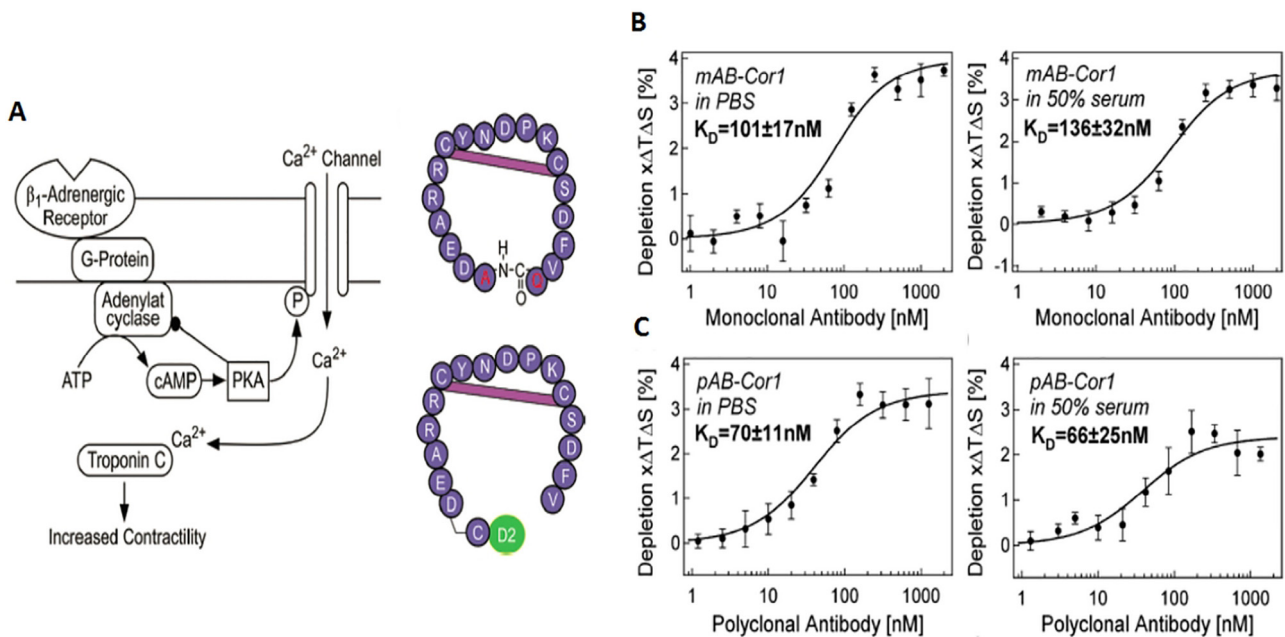


Fig. 3. A) Activation pathway of β_1 -adrenergic receptor (left), synthetic COR1 peptide (right upper), labeled COR1 peptide (right bottom). B) binding curve of monoclonal antibodies to COR1 peptide in PBS buffer and 50% human serum. C) binding curve of polyclonal antibodies to COR1 peptide in PBS buffer and 50% human serum. (Adapted with permission from Ref. [39]).

successfully determined to be $K_d = 10$ nM for (hIFN- γ)-(IFN- γ -antibody) and $K_d = 2.3$ nM for GFP-GBP interactions. MST data of GFP-GBP experiment were compared with data that obtained from quartz crystal microbalance sensor (QCM) and found good agreement between two estimated physical dissociation constants. In this regard, MST is liberating strong physical effect which would be able to estimate the binding events of biomolecules in their native environment and invest this feature in quantification of disease-related biomarker and drug discovery as described by Lip-pok et al. [39]. Whereas, MST was used to quantify the interaction between autoimmune antibodies (β 1-adrenergic receptor autoantibodies) and an artificial peptide antigen (COR1) which is designed to act as a candidate peptide drug in the treatment of dilated cardiomyopathy (Fig. 3A). The affinity of labeled COR1 to monoclonal and polyclonal antibodies was quantified under two different conditions either in buffer or 50% human serum. The binding events were determined as the dissociation constant (K_D). Moreover, binding specificity was confirmed by control experiment using non-specific antibodies (Fig. 3B and C). On the other hand, MST was exploited in different applications of protein-protein interactions to prove the role of some proteins in cancer initiation

or prognosis as well as disease diagnosis. For example, Arbel et al. [40] used MST to investigate the interactions between Bcl-xL proteins and VDAC1 protein (voltage-dependent anion channel-isoform1). This approach was carried out to prove the interaction between Bcl-xL and VDAC1; however, Bcl-xL are overexpressed in cancer and drug resistance might be attributed to their anti-apoptotic activity. MST successfully quantified the binding events of Bcl-xL-VDAC1 ($K_d = 0.67$ μ M). Moreover, VDAC1-based peptides were synthesized to act as a targeted drug in suppression anti-apoptotic activity of Bcl-xL protein. Similarly, Liu et al. [41] used MST to investigate direct interaction of fibrous sheath interacting protein 1 (FSIP1) to human epidermal growth factor receptor 2 (HER2). Where, FSIP1 is a known biomarker correlate to HER2 in growth and metastasis of breast cancer. MST results revealed that binding affinity between intracellular domain (B2) of HER2 and all recombinant FSIP1 fragments, especially (A2) FSIP1 with (B2) HER2 and the estimated $K_d = 0.25$ μ M. Other binding events indicated weak affinity between two molecules. Recently, Löff et al. [42] investigated the interactions between plasma glycoprotein (VWF-CK domain), which is considered an important protein in platelet aggregations during vascular injury, and protein disulfide

Table 1
MST of protein-protein interactions.

Analytical application	Interacting molecules	Binding parameters	Comparative technique	Ref.
Antigen-antibody interactions	Human Interferon-gamma (hIFN- γ) and hIFN- γ antibody	The binding events determined as dissociation constant $K_d = 10 \pm 2$ nM		[28]
Antigen-antibody interactions (small fragment Abs for GFP)	Green fluorescent protein (GFP) with small fragment antibody (GBP)	The binding events determined as dissociation constant $K_d = 2.3 \pm 2.1$ nM	QCM $K_d = 0.63$ nM	[28]
Characterization of antiapoptotic activity for Bcl-xL protein	Voltage-dependent anion channel isoform 1 (VDAC1) and Bcl-xL protein	The binding events determined as dissociation constant $K_d = 0.67$ μ M		[40]
Breast cancer biomarkers	Fibrous sheath interacting protein 1 (FSIP1) and human epidermal growth factor receptor 2 (HER2)	3 FSIP1 isoforms bind to B2 HER2 domain where, A1-B2 $K_d = 0.80 \pm 0.19$ μ M A2-B2 $K_d = 0.25 \pm 0.06$ μ M A3-B2 $K_d = 1.08 \pm 0.25$ μ M		[41]
Functional and structural characterization of glycoprotein.	Von Willebrand factor (VWF) glycoprotein and protein disulfide isomerase -A1 isoform (PDIA1)	The binding events determined as dissociation constant $K_d = 236 \pm 66$ nM	FCS $K_d = 282 \pm 123$ nM	[42]
Characterization of inhibitory functions of synthetic Ca^{2+} channel peptides	Collapsing response mediator protein 2 (CRMP2) and L1 or Ct-dis synthetic peptides	The binding events determined as dissociation constant CRMP2-L1 $K_d = 3$ μ M CRMP2-CT-dis $K_d = 0.64$ μ M		[43]
Discovery of therapeutic peptide	COR1 peptide and autoimmune antibody	The binding events determined as dissociation constant $K_d = 75$ nM		[39]
Protein dimerization	Two monomers of Growth factor receptor-bound protein 2 (Grb2)	The binding events determined as dissociation constant $K_d = 0.66 \pm 0.2$ μ M		[44]
Characterization of cell surface receptor binding to hemagglutinin protein of H5N1 virus	Human or avian receptors and recombinant hemagglutinins (HAs)	Transmissible HA-human receptor $k_d = 12$ mM Wild type HA-human receptor $K_d = 17$ mM Transmissible HA-avian receptor $K_d = 32$ mM		[45]
Protein phosphorylation	Renal water channel aquaporin-2 (AQP2) and lysosomal trafficking regulator-interacting protein -5 (LIP5)	The dissociation constant K_d was determined for different AQP2 mutants in range of 278 nM to 1 μ M in comparison to wild type AQP2-LIP5 $K_d = 191$ nM		[46]
Quantitation of proteins aggregates	α - synuclein oligomer and monomer species (Syn2) and Nano-antibody (Nb Syn2)	The binding events determined as dissociation constant Oligomer-Nb syn2 $K_d = 234 \pm 49$ nM Monomer-Nb syn2 $K_d = 124 \pm 35$ nM		[47]
Characterization of protein inhibition effect in plasma sample	Neutrophil elastase (NE) and α -antitrypsin (AAT)	The K_d was determined in two pool plasma samples FEV1 $\geq 80\%$ $K_d = 500 \pm 100$ nM FEV1 $\leq 50\%$ $K_d = 1300 \pm 250$ nM		[48]
Characterization of lipid metabolic regulations	Aspergillus oryzae acyl-coA binding protein (AoACBP) and palmitoyl-CoA or myristoyl-CoA	The binding events determined as dissociation constant AoACBP-palmitoyl-CoA $K_d = 80$ nM AoACBP-myristoyl-CoA $k_d = 510$ nM		[49]
Protein scaffold	β -trypsin and miniprotein chains	MST binding events determined as dissociation constant β -trypsin-BHV $K_d = 105 \pm 29$ nM β -trypsin-BVB $K_d = 104 \pm 18$ nM β -trypsin-HBH $K_d = 106 \pm 25$ nM	SPRi The binding events determined as dissociation constant β -trypsin-BHV $K_d = 78 \pm 12$ nM β -trypsin-BVB $K_d = 44 \pm 8$ nM β -trypsin-HBH $K_d = 86 \pm 18$ nM	[50]

isomerase isoform A1 (PDIA1) to prove specific and direct interaction and characterize VWF dimerization. MST and fluorescence correlation spectroscopy (FCS) techniques were used to measure binding constant where the dissociation constants that determined by MST and FCS $K_d = 236$ nM and $K_d = 282$ nM, respectively. Different applications [43–50] of MST technique in the characterization of protein-protein interactions are summarized in Table 1.

3.1.2. Protein-small molecule interaction

The binding of small molecule ligands to large protein molecules is crucial in several biological processes. Indeed, MST was merged largely in this field as a novel technique for characterization of protein-small molecules interaction although, quantifications of these interactions are difficult due to lack of significant changes in bulk size or charges of the complex. Thus, the sensitivity of detection is critically affected; however, MST is still capable of detecting the binding events as change in molecular solvation entropy [26,35]. There are several applications for using of MST in measuring small molecules affinity to proteins for therapeutic and technological developments. Drug discovery is the mainstream of different experimental approaches in protein-small molecule interactions, and a large number of studies are consistent with this general aim [51–57]. For instance, Patniak et al. [58] investigated the affinity of candidate small lead compounds to glucocerebrosidase enzymes (GCase). MST approaches were carried out after high throughput screening for a huge number of lead compounds to identify series of compounds that activate GCase, which is considered a good target drug for treatment of Gaucher disease. Moreover, Rogez-Florent et al. [57] investigated the enantioselective affinity of new sulfonamide derivatives to human carbonic anhydrase enzymes. In this substantial approach, MST and SPR were used for the interaction study. On the other hand, the small molecules inhibitory effect was investigated extensively via MST [59–64]. Where, Shang et al. [60] successfully investigated small molecule as inhibitor G-protein-coupled Rho guanine nucleotide exchange factors. MST was used to estimate the binding affinity

between small molecule (Y16) and LARG DH-PH protein and the dissociation constant K_d of ~ 76 nM to be a candidate as an anti-cancer agent. Another example, Welsch et al. [63] recently, investigated multivalent small molecule as an inhibitor for Pan-RAS proteins, which are strongly involved in numerous malignancies. In protein production technology, MST is a robust technique for testing the purified proteins and confirming their functionalities. In this context, Wang et al. produced G protein-coupled receptors using commercial *E. coli* cell-free kits with selected peptides as surfactant [65]. They succeeded to produce milligram quantities of GPCRs; MST was used to confirm the ability of purified receptors to bind with their ligands. Another approach was used by Westermaier et al. [66], who studied the effect of excipients on the initial self-association of therapeutic antibody bevacizumab and breaking protein aggregation. *In silico* screening of several targeted molecules as aggregation breakers, adenosine monophosphate (AMP) showed better aggregation breaking properties (Fig. 4A–C). MST was used to investigate the interactions between AMP and bevacizumab using both MST systems (labeled and label-free MST). Furthermore, the dissociation constant for self-interaction between two bevacizumab monomers was estimated (Fig. 4D and E). In this approach, the labeling process exhibited a great effect on binding events ($K_d = 27.5$ mM) in comparison to label-free MST system ($K_d = 9.59$ mM). Several applications [67–69] such as protein characterizations and protein stability are summarized elsewhere in Table 2.

3.2. MST of nucleic acids interactions

The characterization of nucleic acids (NAs) interactions is highly significant in the life sciences. NAs are a good target in the study of several biological interactions, such as drug discovery and development, protein characterization and catalytic mechanisms. The thermophoretic effect was studied for DNA/RNA stabilities in the early stage [32,70]. For binding events, NAs are a good target in the study of several biological interactions, such as drug discovery

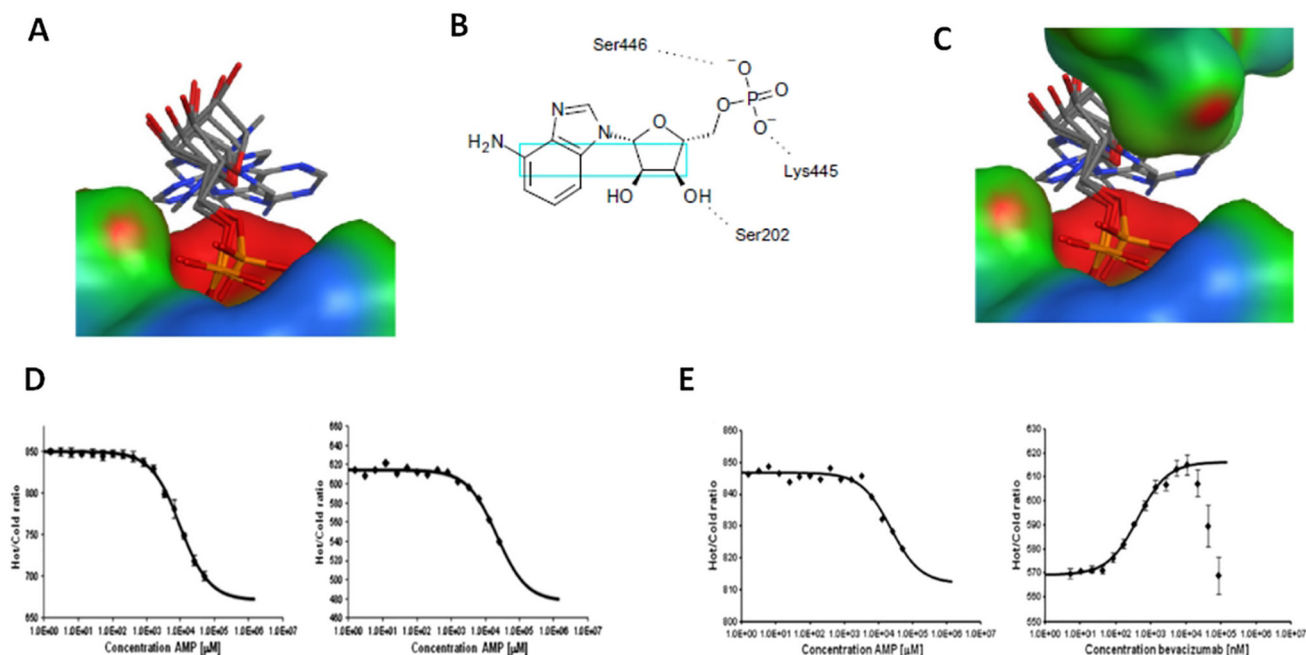


Fig. 4. A) molecular docking of interaction between AMP and bevacizumab monomer. B) AMP chemical structure, dotted line represent suspected binding group to second bevacizumab monomer with specific serine/lysine residues. C) molecular docking of dimer aggregation model in presence of AMP as aggregation breaker. D) binding curves of AMP-Bevacizumab using label-free MST system. E) binding curves of AMP-Bevacizumab with labeling of bevacizumab. (Adapted with permission from [66]).

Table 2
MST of protein-small molecules interactions.

Analytical application	Interacting molecules	MST binding parameters	Comparative techniques	Ref.
Drug discovery of new neutrophil elastase inhibitors	Human neutrophil elastase (HNE) and ursolic acid	Inhibitory constant was determined as K_i HNE-ursolic acid $K_i = 2.72 \pm 0.66 \mu\text{M}$	CE $K_i = 2.81 \pm 0.05 \mu\text{M}$	[51]
Characterization of antiviral activity of small molecules	Tobacco mosaic virus coat protein (TMVCP) and small molecules (chalcone derivatives) in addition to ningnanmycin and ribavirin	TMVCP-7 h $K_d = 9.51 \mu\text{M}$ TMVCP-7r $K_d = 34.8 \mu\text{M}$ TMVCP-7j $K_d = 162 \mu\text{M}$ TMVCP-ningnanmycin $K_d = 9.92 \mu\text{M}$ TMVCP-ribavirin $K_d = 473 \mu\text{M}$	Fluorescence Spectroscopy K_a determined for all binding events in range of 2.57×10^3 to $2.63 \times 10^5 \text{ M}$	[52]
	Tobacco mosaic virus coat protein (TMVCP) and small molecules (glucopyranoside derivatives)	The binding events determined as association constant K_a as follow TMVCP-f6 $K_a = 1.10 \times 10^5 \text{ M}$ TMVCP-f18 $K_a = 1.07 \times 10^4 \text{ M}$ TMVCP-f31 $K_a = 7.69 \times 10^3 \text{ M}$	ITC TMVCP-f6 $K_a = 1.79 \times 10^5 \text{ M}$ TMVCP-f18 $K_a = 2.07 \times 10^4 \text{ M}$ TMVCP-f31 $K_a = 1.76 \times 10^3 \text{ M}$	[53]
Characterization of antiviral activity of small molecules	Tobacco mosaic virus coat protein (TMVCP) and small molecule enantiomers (α -aminophosphonate derivatives)	The binding events determined as association constant K_a as follow: Q enantiomers with TMVCP wild type (WT) TMVCP-Q-R $K_a = 2.03 \times 10^5 \text{ M}$ TMVCP-Q-s $K_a = 8.26 \times 10^3 \text{ M}$ Q-R enantiomer with Different mutants of TMVCP (Q-R)-Q38G $K_a = 2.93 \times 10^4 \text{ M}$. (Q-R)-R90G $K_a = 3.66 \times 10^3 \text{ M}$ (Q-R)-R91G $K_a = 1.71 \times 10^4 \text{ M}$	ITC Q enantiomers with TMVCP wild type (WT) TMVCP-Q-R $K_a = 1.81 \times 10^5 \text{ M}$ TMVCP-Q-s $K_a = 9.89 \times 10^3 \text{ M}$ Q-R enantiomer with Different mutants of TMVCP (Q-R)-Q38G $K_a = 9.10 \times 10^4 \text{ M}$ (Q-R)-R90G $K_a = 8.76 \times 10^3 \text{ M}$ (Q-R)-R91G $K_a = 2.08 \times 10^4 \text{ M}$	[54]
	South rice black-streaked dwarf virus coat protein-P10 gene (SRBSDVCP-P10) and small molecules	The binding events determined as dissociation constant P10-NNM $K_d = 4.27 \mu\text{M}$ P10-F27 $K_d = 7.81 \mu\text{M}$	FT (Fluorescence titration) Binding events determined as K_a P10-NNM $K_a = 6.17 \times 10^5 \text{ M}$ P10-F27 $K_a = 5.75 \times 10^5 \text{ M}$	[55]
Enantioselective inhibition for human carbonic anhydrase II	Human heat-shock protein 90 β (Hsp90) and selected marine alkaloids small molecules	The binding events determined as dissociation constant K_d of four small molecules compounds to Hsp90 in range of 18 – 79 μM in comparison to control inhibitory compound 17-DMAG $K_d = 0.27 \mu\text{M}$		[56]
	Human carbonic anhydrase II (hACII) and different enantiomer of synthetic sulfonamides	The binding events determined as dissociation constant K_d of four enantiomer range of K_d 116 – 697 nM in comparison to reference compound AZA that exhibited highest affinity $K_d = 41 \text{ nM}$	SPR The binding events determined as dissociation constant K_d of four enantiomer range of K_d 152 – 961 nM in comparison to reference compound AZA that exhibited highest affinity $K_d = 38 \text{ nM}$	[57]
Drug discovery and structure activity relationship of small molecule chaperones	Glucocerebrosidase enzyme (GCase) and small molecule chaperone	The binding events determined as dissociation constant GCase – compound 40 $K_d = 8.91 \mu\text{M}$		[58]
Protein aggregate characterization	α -synuclein aggregates (α -syn) and EGCG small molecule	The binding events determined as dissociation constant α -syn fibril-EGCG $K_d = 2.5 \pm 0.4 \mu\text{M}$ α -syn oligomer-EGCG $K_d = 4.3 \pm 0.8 \mu\text{M}$		[47]
Shigella TGT enzyme inhibition	tRNA-guanine transglycosylase of <i>S. mobilis</i> (TGT) and four synthetic small molecules	The binding events determined as dissociation constant Compound 1 $K_d = 1167 \pm 152 \text{ nM}$ Compound 2 $K_d = 1400 \pm 500 \text{ nM}$ Compound 3 $K_d = 18.2 \pm 7.0 \mu\text{M}$ Compound 4 $K_d = 4.08 \text{ nM}$		[59]
Characterization of G-protein coupling inhibitors	LARG protein and Y16 small molecule	The binding events determined as dissociation constant LARG-Y16 $K_d = 76 \text{ nM}$		[60]
Protein stability	Adenylate kinase enzyme (AKE) and (Ap5A) small molecule	The binding events determined as dissociation constant AKE-Ap5A $K_d = 33.4 \pm 4 \text{ nM}$		[61]
Characterization of Protein kinase inhibitors	Human protein kinase 2- α subunit (hCK2 α) and four halogenated benzotriazoles	The binding events determined as dissociation constant hCK2 α -5-BrBt $K_d = 246 \text{ nM}$ hCK2 α -5,6-Br ₂ Bt $K_d = 81 \text{ nM}$ hCK2 α -4,5,6-Br ₃ Bt $K_d = 83 \text{ nM}$ hCK2 α -TBBt $K_d = 45 \text{ nM}$	ITC The binding events determined as dissociation constant hCK2 α -5-BrBt $K_d = 310 \text{ nM}$ hCK2 α -5,6-Br ₂ Bt $K_d = 1170 \text{ nM}$ hCK2 α -4,5,6-Br ₃ Bt $K_d = 990 \text{ nM}$ hCK2 α -TBBt $K_d = 350 \text{ nM}$	[62]
Characterization of RAS Protein inhibitor	Different mutants of KRAS gene and small synthetic molecule (3144)	The binding events determined as dissociation constant (KRAS ^{G12D})-3144 $K_d = 9 \mu\text{M}$	ITC The binding events determined as dissociation constant (KRAS ^{G12D} -GTP)-3144 $K_d = 17.8 \mu\text{M}$	[63]
Characterization of RNR inhibitors	R2 subunit of ribonucleotide reductase (R2-RNR) and different synthetic thiosemicarbazones	The binding events determined as dissociation constant R2-H ₂ L ² $K_d = 2.7 \mu\text{M}$ R2-compound3 $K_d = 3.3 \mu\text{M}$		[64]
Membrane protein production	Olfactory receptor (mOR103-15) and heptanal	The binding events determined as EC50 (mOR103-15)-heptanal EC50 = 9 μM		[65]
Characterization of antibody aggregation	IgG1 antibody (bevacizumab) and AMP	The binding events determined as dissociation constant using two MST systems MST labelFree system Bevacizumab-AMP $K_d = 9.59 \text{ mM}$ MST with labeling system Bevacizumab-AMP $K_d = 22 \text{ mM}$		[66]
Structural characterization of glycoprotein (Avidin)	Avidin (small tetrameric glycoprotein) and hydroxyazobenzene carboxylic acid (HABA)	The binding events determined as dissociation constant Avidin-HABA $K_d = 4.12 \mu\text{M}$		[67]

Table 2 (continued)

Analytical application	Interacting molecules	MST binding parameters	Comparative techniques	Ref.
Characterization of Serum protein binding domain	Bovine serum albumin (BSA) and FITC dye in presence of competitive drugs	The binding events determined as dissociation constant (Warfarin-BSA)-FITC $K_d = 1.24 \mu\text{M}$ (Ibuprofen-BSA)-FITC not determined	FT The binding events determined as association constant (Warfarin-BSA)-FITC $K_a = 2.09 \times 10^6 \text{ M}$ (Ibuprofen-BSA)-FITC $K_a = 0.93 \times 10^6 \text{ M}$	[68]
Characterization of fibrillar protein aggregates	α -synuclein fibrils (α -Syn) and Tau fibrils against small molecules	The binding events determined as dissociation constant α -synuclein - small molecules K_d range of 285–3100 nM -Tau - small molecules K_d range of 2–123 nM		[69]

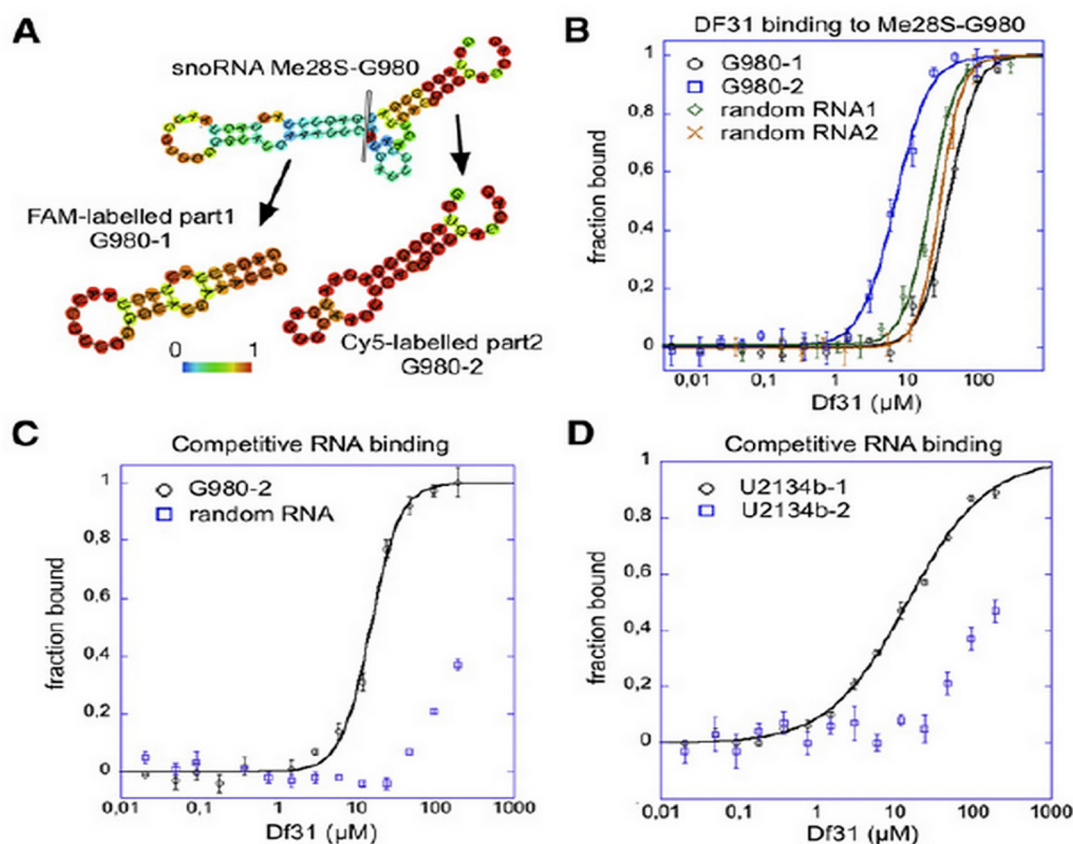


Fig. 5. A) represent two different labeled fragments (G980 part 1 and G980 part 2) of synthesized snoRNA species Me28S-G980. B) binding curve of Df31-Me28S-G980 in presence of nonspecific RNA molecules. C) competitive binding curve of Df31-G980-2 in presence of nonspecific molecules RNA. D) competitive binding curve of Df31-Me28S-U2134b in presence of nonspecific RNA molecules. (Adapted with permission from Ref. [71]).

and development, protein characterization and catalytic mechanisms. For instance, Schubert et al. [71] characterized the role of small nucleolar RNA (snoRNA) and chromatin associated protein known as decondensation factor 31 (Df31) in maintaining accessibility of higher-order structure of chromatin. MST was successfully used to evaluate the binding affinity of Df31 toward RNA in the presence of other nucleic acids competitors. Additionally, the affinity of Df31 toward different histone molecules (major components of chromatin) was investigated as well as of direct interaction between Df31 and snoRNA species (Me28S-U2134b, Me28S-G980) in order to prove the role of snoRNA and Df31 in chromatin as high-order structure mediators. Df31 exhibited higher affinity toward snoRNAs fragments in presence of random RNA fragments (Fig. 5). Similarly, Zillner et al. [72] investigated the binding event for specific peptides known as (AT-hook) of Tip5 protein (major regulatory subunit in nucleolar remodeling complex) with ribozyme DNA (rDNA) in order to identify the regulatory function of Tip5 protein in regulation of higher-order rDNA chromatin structure. MST results revealed weak affinity in comparison to control

(HMGA1). Furthermore, Gaffarogullari et al. [73] used MST to investigate the interaction of small-molecule substrate to RNA enzyme known as Diels-Alderase ribozyme (DAse) while, previous approaches using FCS technique failed to quantitate the binding event due to interference with small-molecule labeling procedures for maleimide dienophiles substrate. MST approach used via two experimental sets: the first analyzed the binding interactions between DAse and diene substrates that was successfully investigated by FCS to access the suitability of MST, which exhibited good agreement with FCS measurements. The second experimental set investigated the interaction between DAse and maleimide dienophile substrates. MST but not FCS was reliably used in the determination of the dissociation constant for DAse-maleimide dienophile substrates. MST of nucleic interactions are summarized in Table 3.

3.3. MST nucleic acids aptamer interactions

Among middle molecular weight biomolecules, aptamer gained significant attention in recent years due to high-binding affinity

Table 3
MST of nucleic acids and nucleic acid aptamers interactions.

Analytical application	Interacting molecules	MST binding parameters	Comparative techniques	Ref.
<i>MST of nucleic acids interactions</i>				
Characterization of high order structure of Chromatin	Decondensation factor 31 (DF31) protein and single or double strand RNA, histone molecules and small nucleolar RNA (snoRNA)	The binding events determined as K_d Df31 - nonspecific RNA determined as $K_d = 24 \mu\text{M}$ Df31-histone H3 $K_d = 1.5 \mu\text{M}$ Df31- histone H4 $K_d = 12 \mu\text{M}$ Df31 - snoRNA species K_d range of 7–14.5 μM		[71]
Characterization of chromatin regulatory functions	AT-hook peptides and rDNA	The binding events determined as EC50 where, EC50 of different AT-hook peptide bound to rDNA in range of 1.4–7.9 μM		[72]
Ribozyme catalysis mechanism	Diels-Alderase ribozyme (DAse) and small molecules anthracene and maleimide dienophiles	MST binding events determined as K_d (DAse)-9-DAP $K_d = 32 \mu\text{M}$ (DAse)-9-AB $K_d = 1764 \mu\text{M}$ (DAse)-1-AB $K_d = 215 \mu\text{M}$	FCS FCS binding events determined as K_d (DAse)-9-DAP $K_d = 12 \mu\text{M}$ (DAse)-9-AB $K_d = 1210 \mu\text{M}$ (DAse)-1-AB $K_d = 300 \mu\text{M}$	[73]
<i>MST of nucleic acid aptamers interactions</i>				
Characterization of aptamer interaction to small molecules	ATP aptamer and ATP, AMP, ADP, SAM, dATP, Adenine, CTP and GTP	The binding events of ATP determined as EC50 and compared to reported methods -Aptamer-ATP EC50 = 34.4 μM - other ligands EC50 in range of 28–68 μM	ATP-aptamer interactions compared to Centrifugal filter $K_d = 6 \mu\text{M}$ Isocratic elution $K_d = 13 \mu\text{M}$	[38]
Characterization of aptamer binding properties in different media	Aptamer against thrombin, ATP and AMP	The binding events was determined as K_d for Aptamer-thrombin interactions where, $K_d = 30 \text{ nM}$ The binding events was determined as EC50 for Aptamer-ATP/AMP interactions. Aptamer-ATP EC50 = 60 μM Aptamer-AMP EC50 = 87 μM		[77]
Ochratoxin A probing	Aptamer 1.12.2 and ochratoxin A (OTA) in different mixture	The binding events was determined as K_d Aptamer-OTA in different mixture K_d in range of 2.60–4.81 μM		[78]
Steroid testosterone probing	Aptamer and Testosterone 5 (T5) candidate	The binding events of Aptamer-T5 was determined as $K_d = 5.7 \text{ nM}$	Apta PCR affinity assay (APAA) Aptamer - T5 $K_d = 4.0 \text{ nM}$	[79]
Cholic acid probing (diagnostic development)	Aptamer and cholic acid (CA)	The binding event was determined as dissociation constant Aptamer-CA $K_d = 12.6 \mu\text{M}$		[80]

and specificity. Aptamers consist of single- strand oligonucleotide or peptide sequences which are selected and generated in vitro by a selection process known as the systemic evolution of ligands by exponential enrichment (SELEX). Today, aptamers are widely used either as diagnostic or therapeutic agents [74–76]. In the earlier evaluation of MST, aptamer binding studies were carried out with different targeted molecules such as proteins and small molecules. Baaske et al. used MST technique to quantify the buffer dependence of aptamer binding [77]. Two approaches were performed for aptamers interaction with macro/micro molecule partners. The first approach was designed to study aptamer-protein interaction where thrombin (37 kDa) was selected as a targeted protein. Aptamer-protein interactions were carried out in pure buffer system and in 10% and 50% human serum. The binding was quantified as dissociation constant $K_d = 30 \text{ nM}$ in a pure buffer system, which agrees with reported method while, in 10% and 50% human serum the binding was fitted with Hill equation whereas EC50 = 670 nM and 720 nM, respectively. The second approach was carried out to investigate aptamer-small molecules interactions: AMP and ATP were selected as targeted molecules to bind with specific aptamer. The binding was quantified by Hill equation as EC50 for AMP = 87 μM and ATP = 60 μM , which agreed with reported values. In this context, Entzian et al. [38] applied another approach to investigate aptamer-small molecule interaction where ATP, AMP, ADP, SAM, dATP, Adenine, CTP and GTP were selected as a targeted small molecules. The binding affinity fitted well with Hill equation as EC50 in range of 28–68 μM except for CTP and GTP that didn't exhibit affinity to the aptamer. In contrast, aptamers were exploited as a bio-probe for such targeted molecules [78–80]. Schax et al. [78] in another application to MST of aptamer interaction, used specific aptamer as a probe for ochratoxin A contaminants in beer, coffee, juice, and wine. The method was successful in determining ochratoxins A residuals in all selected samples and the determined K_d values were in low micromolar concentrations. Furthermore, Skouridou et al. [79] used specific aptamer (T5)

as a probe for testosterone (anabolic steroid) interactions. The specific aptamer (T5) exhibited higher affinity to testosterone among other candidates using MST pic instrument. The dissociation constant determined with MST $K_d = 5.7 \text{ nM}$ was in agreement with K_d values that obtained from apta-PCR affinity assay ($K_d = 4 \text{ nM}$). Recently, Zhu et al. [80] used MST to evaluate specifically designed aptamer for cholic acid binding, exploited in developing new biosensors for cholic acid detections used as aptamer-gold nanoprobe. MST for aptamer interactions are summarized in Table 3.

3.4. MST of miscellaneous applications

In this section, several applications of MST are discussed, such as liposomal interactions, enzyme-metal ions interaction, and MST in metal ions chelation, which are significant interactions and directly involved in biological systems. MST of liposomal interactions were studied by Bogaart et al. [81]. In this study, MST was used to quantify the binding of phosphatidylinositol 4,5-Bisphosphate (PIP₂) and Ca²⁺ to synaptotagmin-1. Thus, the characterization of this binding event is crucial to understanding the releasing mechanism of neurotransmitters. MST proved that PIP₂ binding to C2B domain of synaptotagmin-1 to increase the sensitivity of synaptotagmin-1 toward Ca²⁺. Moreover, MST was used to investigate protein-metal ions binding events due to high sensitivity to tiny conformational changes of targeted macromolecules that lead to significant changes in thermophoretic properties. Wienken et al. proved the binding affinity to Ca²⁺ receptor calmodulin (CaM) with Ca²⁺ and Mg²⁺. MST quantitated the dissociation constant for CaM-Ca²⁺ ($K_d = 2.8 \mu\text{M}$) while no binding events was detected for Mg²⁺ [28]. Similarly, Pang et al. [82] used MST to investigate the interaction between oxalate oxidase (OxOx) and selected metal ions (Ca²⁺, Fe³⁺). MST was used to investigate binding affinity between OxOx and metal ions in different pH systems. Next, inhibitory effect of metal ions for OxOx was evaluated using circular dichromism.

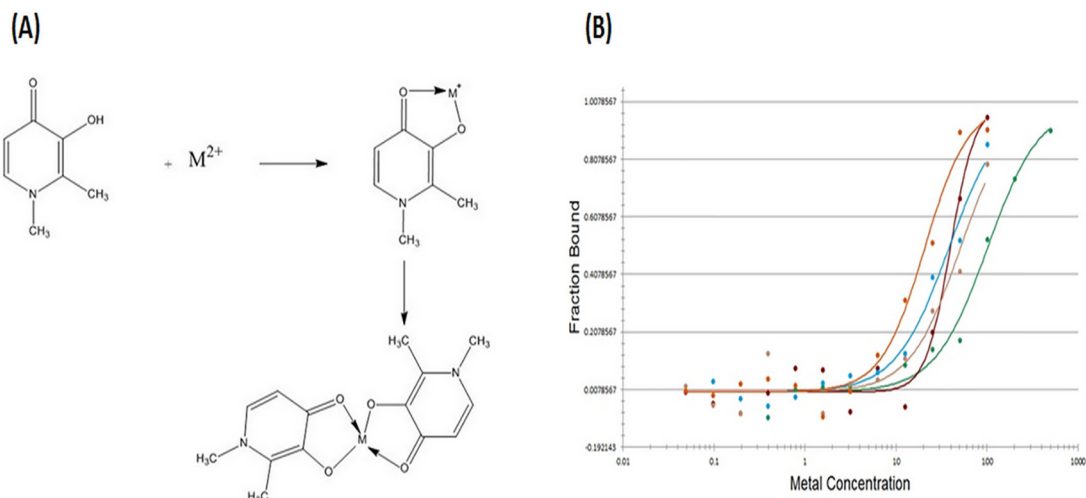


Fig. 6. A) represent scheme of interaction mechanism between CP20 and divalent essential metal ions. B) Saturation curves for CP20–metal ions. Green curve indicates Ni^{2+} ions ($\text{EC}_{50} = 101.1 \pm 22.70$), brown curve indicates Zn^{2+} ions ($\text{EC}_{50} = 39.5 \pm 4.90$), blue curve indicates Cu^{2+} ions ($\text{EC}_{50} = 38.1 \pm 3.39$), gray curve indicates Co^{2+} ions ($\text{EC}_{50} = 51.1 \pm 6.86$), and red curve indicates Fe^{3+} ions ($\text{EC}_{50} = 20.6 \pm 3.34$). (Adapted with permission from Ref. [83]). (For interpretation of the references to colour in this figure legend, the reader is referred to the web version of this article.)

The binding affinity of OxOx toward Fe^{3+} was pH dependent whereas interaction was very weak at pH 3.5 ($K_d = 2.2$ mM) and, with increasing pH to 6.0, the interaction dramatically increased ($K_d = 0.49$ mM) while Ca^{2+} didn't exhibit any binding. Recently, Asmari et al. [83] investigated the binding of iron-chelator deferoxamine (CP20) to different essential metal ions. MST was used to screen the affinity of CP20 towards Fe^{3+} , Cu^{2+} , Zn^{3+} , Co^{2+} , Ni^{2+} , Mn^{2+} , Mg^{2+} and Ca^{2+} . In this approach, under the constant MST conditions the affinity of divalent metal ions to CP20 was varied where Cu^{2+} and Zn^{2+} has a higher affinity to bind with CP20 than other divalent metal ions (Fig. 6), which agrees with previous reports. Mg^{2+} and Ca^{2+} did not show any binding affinity to CP20, which are the most abundant metal ions in human body. MST data were successfully fitted with Hill equations and EC_{50} was successfully estimated. The system cooperativity was observed.

4. Conclusion

This review describes and summarizes recent studies of MST techniques with biomolecular interactions. MST was successfully used to analyse a wide range of molecules since the factors that affect molecular thermophoresis do not depend solely on a change of molecular size, which is difficult to detect in some cases but so are any changes hydration shell or charges. The technical and experimental approaches, as well as a comprehensive review of theoretical background, are discussed in detail. Indeed, several methodological challenges in other competitive techniques were overcome in the MST system such as immobilization procedures, high sample volumes, long time measurements, and simple handling. We discussed in detail several applications of binding studies using MST for protein–protein interactions, protein–small molecules interaction, nucleic acids interactions, aptamer interaction and non-categorized interaction studies, which revealed wide application of the technique in the characterization of biomolecular interaction.

Acknowledgment

We gratefully acknowledge the Saudi Arabian Cultural Office in Berlin and King Khalid University for supporting our work by a grant to M. Asmari.

References

- [1] M. Citartan, S.C.B. Gopinath, J. Tominaga, T.-H. Tang, Label-free methods of reporting biomolecular interactions by optical biosensors, *Analyst* 138 (2013) 3576–3592.
- [2] X. Zheng, Z. Li, S. Beeram, M. Podariu, R. Matsuda, E.L. Pfaunmiller, C.J. White, N.T. Carter, D.S. Hage, Analysis of biomolecular interactions using affinity microcolumns: a review, *J. Chromatogr. B Anal. Technol. Biomed. Life Sci.* 968 (2014) 49–63.
- [3] X. Zheng, C. Bi, Z. Li, M. Podariu, D.S. Hage, Analytical methods for kinetic studies of biological interactions: a review, *J. Pharm. Biomed. Anal.* 113 (2015) 163–180.
- [4] C. Bi, R. Matsuda, C. Zhang, Z. Isingizwe, W. Clarke, D.S. Hage, Studies of drug interactions with alpha1-acid glycoprotein by using on-line immunoelectrochromatography and high-performance affinity chromatography, *J. Chromatogr. A.* 1519 (2017) 64–73.
- [5] Z. Li, D.S. Hage, Analysis of stereoselective drug interactions with serum proteins by high-performance affinity chromatography: a historical perspective, *J. Pharm. Biomed. Anal.* 144 (2017) 12–24.
- [6] Y. Li, B. He, L. Hu, X. Huang, Z. Yun, R. Liu, Q. Zhou, G. Jiang, Characterization of mercury-binding proteins in human neuroblastoma SK-N-SH cells with immobilized metal affinity chromatography, *Talanta* 178 (2017) 811–817.
- [7] H.A. Alhazmi, M. Nachbar, H.M. Albishri, D.A. El-Hady, S. Redweik, S. El Deeb, H. Wätzig, A comprehensive platform to investigate protein–metal ion interactions by affinity capillary electrophoresis, *J. Pharm. Biomed. Anal.* 107 (2015) 311–317.
- [8] M. Nachbar, S. El Deeb, M. Mozafari, H.A. Alhazmi, L. Preu, S. Redweik, W.D. Lehmann, H. Wätzig, Ca^{2+} -complex stability of GAPAGLIVPY peptide in gas and aqueous phase, investigated by affinity capillary electrophoresis and molecular dynamics simulations and compared to mass spectrometric results, *Electrophoresis* 37 (2016) 744–751.
- [9] M. Mozafari, S. Balasubramaniam, L. Preu, S. El Deeb, C.G. Reiter, H. Wätzig, Using affinity capillary electrophoresis and computational models for binding studies of heparinoids with p-selectin and other proteins, *Electrophoresis* 38 (2017) 1560–1571.
- [10] Y. Mano, K. Kusano, A validated LC-MS/MS method of total and unbound lenvatinib quantification in human serum for protein binding studies by equilibrium dialysis, *J. Pharm. Biomed. Anal.* 114 (2015) 82–87.
- [11] A.K. Sarker, P.J. Cashin, V.K. Balakrishnan, K. Exall, H.K. Chung, E. Buncel, R.S. Brown, Determining binding of sulfonamide antibiotics to CTAB micelles using semi-equilibrium dialysis, *Sep. Purif. Technol.* 162 (2016) 134–141.
- [12] Z. Ye, C. Zetterberg, H. Gao, Automation of plasma protein binding assay using rapid equilibrium dialysis device and Tecan workstation, *J. Pharm. Biomed. Anal.* 140 (2017) 210–214.
- [13] N.S. El-Safory, G.C. Lee, C.K. Lee, Characterization of hyaluronate lyase from *Streptococcus pyogenes* bacteriophage H4489A, *Carbohydr. Polym.* 84 (2011) 1182–1191.
- [14] P. Kundu, N. Chattopadhyay, Interaction of a bioactive pyrazole derivative with calf thymus DNA: deciphering the mode of binding by multi-spectroscopic and molecular docking investigations, *J. Photochem. Photobiol. B Biol.* 173 (2017) 485–492.
- [15] J.J. Mittag, B. Kneidl, T. Preiß, M. Hossann, G. Winter, S. Wuttke, H. Engelke, J.O. Rädler, Impact of plasma protein binding on cargo release by thermosensitive liposomes probed by fluorescence correlation spectroscopy, *Eur. J. Pharm. Biopharm.* 119 (2017) 215–223.

- [16] M. Chatterjee, B. Nöding, E.A.J. Willemse, M.J.A. Koel-Simmelink, W.M. van der Flier, D. Schild, C.E. Teunissen, Detection of contactin-2 in cerebrospinal fluid (CSF) of patients with Alzheimer's disease using Fluorescence Correlation Spectroscopy (FCS), *Clin. Biochem.* 18 (2017) 1061–1066.
- [17] H. Yang, Y. Huang, J. He, S. Li, B. Tang, H. Li, Interaction of lafutidine in binding to human serum albumin in gastric ulcer therapy: STD-NMR, WaterLOGSY-NMR, NMR relaxation times, Tr-NOESY, molecule docking, and spectroscopic studies, *Arch. Biochem. Biophys.* 606 (2016) 81–89.
- [18] S. Wiesner, R. Sprangers, Methyl groups as NMR probes for biomolecular interactions, *Curr. Opin. Struct. Biol.* 35 (2015) 60–67.
- [19] F. Fathi, J. Ezzati Nazhad Dolatanbadi, M.-R. Rashidi, Y. Omid, Kinetic studies of bovine serum albumin interaction with PG and TBHQ using surface plasmon resonance, *Int. J. Biol. Macromol.* 91 (2016) 1045–1050.
- [20] B. Sikarwar, V.V. Singh, P.K. Sharma, A. Kumar, D. Thavaselvam, M. Boopathi, B. Singh, Y.K. Jaiswal, DNA-probe-target interaction based detection of *Brucella melitensis* by using surface plasmon resonance, *Biosens. Bioelectron.* 87 (2017) 964–969.
- [21] E. Fabini, U.H. Danielson, Monitoring drug-serum protein interactions for early ADME prediction through Surface Plasmon Resonance technology, *J. Pharm. Biomed. Anal.* 144 (2017) 188–194.
- [22] M. Braia, D. Loureiro, G. Tubio, M.E. Lienqueo, D. Romanini, Interaction between trypsin and alginate: an ITC and DLS approach to the formation of insoluble complexes, *Colloids Surf. B Biointerf.* 155 (2017) 507–511.
- [23] L.Y. Yang, S.Y. Hua, Z.Q. Zhou, G.C. Wang, F.L. Jiang, Y. Liu, Characterization of fullerene-protein interactions and an extended investigation on cytotoxicity, *Colloids Surf. B Biointerf.* 157 (2017) 261–267.
- [24] Z. Li, Z. Wang, N. Wang, X. Han, W. Yu, R. Wang, J. Chang, Identification of the binding between three fluoronucleoside analogues and fat mass and obesity-associated protein by isothermal titration calorimetry and spectroscopic techniques, *J. Pharm. Biomed. Anal.* 149 (2018) 290–295.
- [25] J. Ma, N. Liu, L. Li, X. Ma, X. Li, Y. Liu, Y. Li, Z. Zhou, Z. Gao, An evaluation assay for thymine-mercuric-thymine coordination in the molecular beacon-binding system based on microscale thermophoresis, *Sensors Actuators B Chem.* 252 (2017) 680–688.
- [26] S.A.I. Seidel, P.M. Dijkman, W.A. Lea, G. van den Bogaart, M. Jerabek-Willemsen, A. Lazić, J.S. Joseph, P. Srinivasan, P. Baaske, A. Simeonov, I. Katritch, F.A. Melo, J.E. Ladbury, G. Schreiber, A. Watts, D. Braun, S. Dühr, Microscale thermophoresis quantifies biomolecular interactions under previously challenging conditions, *Methods* 59 (2013) 301–315.
- [27] Y. Mao, L. Yu, R. Yang, C. Ma, L.B. Qu, P.D.B. Harrington, New insights into side effect of solvents on the aggregation of human islet amyloid polypeptide 11–20, *Talanta* 148 (2016) 380–386.
- [28] C.J. Wienken, P. Baaske, U. Rothbauer, D. Braun, S. Dühr, Protein-binding assays in biological liquids using microscale thermophoresis, *Nat. Commun.* 1 (2010) 1–7.
- [29] D. Braun, A. Libchaber, Trapping of DNA by thermophoretic depletion and convection, *Phys. Rev. Lett.* 89 (18803) (2002) 1–4.
- [30] R. Piazza, B. Triulzi, D. Fisica, *Case Protein Solutions* 6 (2004) 1616–1622.
- [31] S. Iacopini, R. Piazza, Thermophoresis in protein solutions, *Europhys. Lett.* 63 (2007) 247–253.
- [32] P. Reineck, C.J. Wienken, D. Braun, Thermophoresis of single stranded DNA, *Electrophoresis* 31 (2010) 279–286.
- [33] S.A.I. Seidel, C.J. Wienken, S. Geissler, M. Jerabek-Willemsen, S. Dühr, A. Reiter, D. Trauner, D. Braun, P. Baaske, Label-free microscale thermophoresis discriminates sites and affinity of protein-ligand binding, *Angew. Chemie - Int. Ed.* 51 (2012) 10656–10659.
- [34] M. Jerabek-Willemsen, C.J. Wienken, D. Braun, P. Baaske, S. Dühr, Molecular interaction studies using microscale thermophoresis, *Assay Drug Dev. Technol.* 9 (2011) 342–353.
- [35] M. Jerabek-Willemsen, T. Andre, R. Wanner, H.M. Roth, S. Dühr, P. Baaske, D. Breitsprecher, MicroScale Thermophoresis: Interaction analysis and beyond, *J. Mol. Struct.* 1077 (2014) 101–113.
- [36] T. Schubert, G. Längst, Studying Epigenetic Interactions Using MicroScale Thermophoresis (MST) 3 (2015) 370–380.
- [37] H. Wätzig, I. Oltmann-Norden, F. Steinicke, H.A. Alhazmi, M. Nachbar, D.A. El-Hady, H.M. Albishri, K. Baumann, T. Exner, F.M. Böckler, S. El Deeb, Data quality in drug discovery: the role of analytical performance in ligand binding assays, *J. Comput. Aided. Mol. Des.* (2015) 847–856.
- [38] C. Entzian, T. Schubert, Studying small molecule-aptamer interactions using MicroScale Thermophoresis (MST), *Methods* 97 (2016) 27–34.
- [39] S. Lippok, S.A.I. Seidel, S. Dühr, K. Uhland, H.-P. Holthoff, D. Jenne, D. Braun, Direct detection of antibody concentration and affinity in human serum using microscale thermophoresis, *Anal. Chem.* 84 (2012) 3523–3530.
- [40] N. Arbel, D. Ben-Hail, V. Shoshan-Barmatz, Mediation of the antiapoptotic activity of Bcl-xL protein upon interaction with VDAC1 protein, *J. Biol. Chem.* 287 (2012) 23152–23161.
- [41] T. Liu, H. Zhang, L. Sun, D. Zhao, P. Liu, M. Yan, N. Zaidi, S. Izadmehr, A. Gupta, W. Abu-Amer, M. Luo, J. Yang, X. Ou, Y. Wang, X. Bai, Y. Wang, M.I. New, M. Zaidi, T. Yuen, C. Liu, W.S. El-Deiry, C. Huang, H.M. Shepard, FSIP1 binds HER2 directly to regulate breast cancer growth and invasiveness, *Proc. Natl. Acad. Sci. U.S.A.* 29 (2017) 3683–3688.
- [42] A. Löf, J.P. Müller, M. Benoit, M.A. Brehm, Biophysical approaches promote advances in the understanding of von Willebrand factor processing and function, *Adv. Biol. Regul.* 63 (2017) 81–91.
- [43] S.M. Wilson, B.S. Schmutzler, J.M. Brittain, E.T. Dustrude, M.S. Ripsch, J.J. Pellman, T.S. Yeum, J.H. Hurley, C.M. Hingtgen, F.A. White, R. Khanna, Inhibition of transmitter release and attenuation of anti-retroviral-associated and tibial nerve injury-related painful peripheral neuropathy by novel synthetic Ca²⁺ channel peptides, *J. Biol. Chem.* 287 (2012) 35065–35077.
- [44] C.C. Lin, F.A. Melo, R. Ghosh, K.M. Suen, L.J. Stagg, J. Kirkpatrick, S.T. Arold, Z. Ahmed, J.E. Ladbury, Inhibition of basal FGF receptor signaling by dimeric Grb2, *Cell* 149 (2012) 1514–1524.
- [45] X. Xiong, P.J. Coombs, S.R. Martin, J. Liu, H. Xiao, J.W. McCauley, K. Locher, P.A. Walker, P.J. Collins, Y. Kawaoka, J.J. Skehel, S.J. Gamblin, Receptor binding by a ferret-transmissible H5 avian influenza virus, *Nature* 497 (2013) 392–396.
- [46] J.V. Roche, S. Survery, S. Kreida, V. Nesverova, H. Ampah-Korsah, M. Gourdon, P.M.T. Deen, S. Törnroth-Horsefield, Phosphorylation of human aquaporin 2 (AQP2) allosterically controls its interaction with the lysosomal trafficking protein LIP5, *J. Biol. Chem.* 292 (2017) 14636–14648.
- [47] M. Wolff, J.J. Mittag, T.W. Herling, E. De Genst, C.M. Dobson, T.P.J. Knowles, D. Braun, A.K. Buell, Quantitative thermophoretic study of disease-related protein aggregates, *Sci. Rep.* 6 (2016) 22829–22838.
- [48] T. Dau, E.V. Edeleva, S.A.I. Seidel, R.A. Stockley, D. Braun, D.E. Jenne, Quantitative analysis of protease recognition by inhibitors in plasma using microscale thermophoresis, *Sci. Rep.* 6 (2016) 35413–35419.
- [49] Q. Hao, X. Liu, G. Zhao, L. Jiang, M. Li, B. Zeng, Recombinant expression, purification, and characterization of an acyl-CoA binding protein from *Aspergillus oryzae*, *Biotechnol. Lett.* 38 (2016) 519–525.
- [50] S. Sankaran, I. Stojanovic, A. Barendregt, A.J.R. Heck, R.B.M. Schasfoort, P. Jonkheijm, Scaffolding of cysteine-stabilized miniproteins, *ChemistrySelect* 5 (2016) 1039–1046.
- [51] F. Syntia, R. Nehm, B. Claude, P. Morin, Human neutrophil elastase inhibition studied by capillary electrophoresis with laser induced fluorescence detection and microscale thermophoresis, *J. Chromatogr. A* 1431 (2016) 215–223.
- [52] L.R. Dong, D.Y. Hu, Z.X. Wu, J.X. Chen, B.A. Song, Study of the synthesis, antiviral bioactivity and interaction mechanisms of novel chalcone derivatives that contain the 1,1-dichloropropene moiety, *Chinese Chem. Lett.* 28 (2017) 1566–1570.
- [53] M. Chen, D. Hu, X. Li, S. Yang, W. Zhang, P. Li, B. Song, Antiviral activity and interaction mechanisms study of novel glucopyranoside derivatives, *Bioorganic Med. Chem. Lett.* 25 (2015) 3840–3844.
- [54] W. Zhang, X. Li, G. Zhang, Y. Ding, L. Ran, L. Luo, J. Wu, D. Hu, B. Song, Binding interactions between enantiomeric -aminophosphonate derivatives and tobacco mosaic virus coat protein, *Int. J. Biol. Macromol.* 94 (2017) 603–610.
- [55] L. Ran, Y. Ding, L. Luo, X. Gan, X. Li, Y. Chen, D. Hu, B. Song, Interaction research on an antiviral molecule that targets the coat protein of southern rice black-streaked dwarf virus, *Int. J. Biol. Macromol.* 103 (2017) 919–930.
- [56] K.-E. Lillsunde, T. Tomašič, D. Kikelj, P. Tammela, Marine alkaloid oroidin analogues with antiviral potential: a novel class of synthetic compounds targeting the cellular chaperone Hsp90, *Chem. Biol. Drug Des.* 6 (2017) 1147–1154.
- [57] T. Rogez-Florent, C. Foulon, A.S. Drucbert, N. Schifano, P. Six, S. Devassine, P. Depreux, P.M. Danzé, L. Goossens, C. Danel, J.F. Goossens, Chiral separation of new sulfonamide derivatives and evaluation of their enantioselective affinity for human carbonic anhydrase II by microscale thermophoresis and surface plasmon resonance, *J. Pharm. Biomed. Anal.* 137 (2017) 113–122.
- [58] S. Patnaik, W. Zheng, J.H. Choi, O. Motabar, N. Southall, W. Westbroek, W.A. Lea, A. Velayati, E. Goldin, E. Sidransky, W. Leister, J.J. Marugan, Discovery, structure – activity relationship, and biological evaluation of noninhibitory small molecule chaperones of glucocerebrosidase, *J. Med. Chem.* 55 (2012) 5734–5748.
- [59] F. Immekus, L.J. Barandun, M. Betz, F. Debaene, S. Petiot, S. Sanglier-Cianferani, K. Reuter, F. Diederich, G. Klebe, Launching spiking ligands into a protein-protein interface: a promising strategy to destabilize and break interface formation in a tRNA modifying enzyme, *ACS Chem. Biol.* 8 (2013) 1163–1178.
- [60] X. Shang, F. Marchioni, C.R. Evelyn, N. Sipes, X. Zhou, W. Seibel, M. Wortman, Y. Zheng, Small-molecule inhibitors targeting G-protein-coupled Rho guanine nucleotide exchange factors, *Proc. Natl. Acad. Sci.* 110 (2013) 3155–3160.
- [61] H. Mazal, H. Aviram, I. Riven, G. Haran, Effect of ligand binding on a protein with a complex folding landscape, *Phys. Chem. Chem. Phys.* (2017), <https://doi.org/10.1039/C7CP03327C>.
- [62] M. Winiewska, E. Bugajska, J. Poznanski, ITC-derived binding affinity may be biased due to titrant (nano)-aggregation. Binding of halogenated benzotriazoles to the catalytic domain of human protein kinase CK2, *PLoS One* (2017) 1–15.
- [63] M.E. Welsch, A. Kaplan, J.M. Chambers, M.E. Stokes, P.H. Bos, A. Zask, Y. Zhang, M. Sanchez-Martin, M.A. Badgley, C.S. Huang, T.H. Tran, H. Akkiraju, L.M. Brown, R. Nandakumar, S. Cremers, W.S. Yang, L. Tong, K.P. Olive, A. Ferrando, B.R. Stockwell, Multivalent small-molecule Pan-RAS inhibitors, *Cell* 168 (2017) 878–889.
- [64] M.F. Zaltariov, M. Hammerstad, H.J. Arabshahi, K. Jovanovi, K.W. Richter, M. Cazacu, S. Shova, M. Balan, N.H. Andersen, S. Radulovic, J. Reynisson, K.K. Andersson, V.B. Arion, New iminodiacetate-thiosemicarbazone hybrids and their Copper(II) complexes are potential ribonucleotide reductase R2 inhibitors with high antiproliferative activity, *Inorg. Chem.* 56 (2017) 3532–3549.
- [65] X. Wang, K. Corin, P. Baaske, C.J. Wienken, M. Jerabek-Willemsen, S. Dühr, D. Braun, S. Zhang, Peptide surfactants for cell-free production of functional G protein-coupled receptors, *Proc. Natl. Acad. Sci. U.S.A.* 108 (2011) 9049–9054.
- [66] Y. Westermaier, M. Veurink, T. Riis-Johannessen, S. Guinchard, R. Gurny, L. Scapozza, Identification of aggregation breakers for bevacizumab (Avastin®) self-association through similarity searching and interaction studies, *Eur. J. Pharm. Biopharm.* 85 (2013) 773–780.

- [67] P. Strzelczyk, G. Bujacz, Crystal structure and ligand affinity of avidin in the complex with-hydroxyazobenzene-2-carboxylic acid, *J. Mol. Struct.* 1109 (2016) 232–238.
- [68] Y. Mao, L. Yu, R. Yang, L. Qu, P.D.B. Harrington, A novel method for the study of molecular interaction by using microscale thermophoresis, *Talanta* 132 (2015) 894–901.
- [69] E. Fisher, Y. Zhao, R. Richardson, A.K. Buell, F.I. Aigbirhio, G. Toth, Detection and characterization of small molecule interactions with fibrillar protein aggregates using microscale thermophoresis detection and characterization of small molecule interactions with fibrillar protein aggregates using microscale thermophoresis, *ACS Chem. Neurosci.* 8 (2017) 2088–2095.
- [70] C.J. Wienken, P. Baaske, S. Duhr, D. Braun, Thermophoretic melting curves quantify the conformation and stability of RNA and DNA, *Nucleic Acids Res.* 8 (2011) 1–10.
- [71] T. Schubert, M.C. Pusch, S. Diermeier, V. Benes, E. Kremmer, A. Imhof, G. Längst, Df31 protein and snoRNAs maintain accessible higher-order structures of chromatin, *Mol. Cell.* 48 (2012) 434–444.
- [72] K. Zillner, M. Filarsky, K. Rachow, M. Weinberger, G. Längst, A. Németh, Large-scale organization of ribosomal DNA chromatin is regulated by Tip5, *Nucleic Acids Res.* 41 (2013) 5251–5262.
- [73] E.C. Gaffarogullari, A. Krause, J. Balbo, D.-P. Herten, A. Jäschke, Microscale thermophoresis provides insights into mechanism and thermodynamics of ribozyme catalysis, *RNA Biol.* 10 (2013) 1815–1821.
- [74] Y. Nakamura, Aptamers as therapeutic middle molecules, *Biochimie* (2017). In press.
- [75] L. Civit, S.M. Taghdisi, A. Jonczyk, S. Hassel, C. Grober, M. Blank, H.J. Stunden, M. Beyer, J. Schultze, E. Latz, G. Mayer, Systematic evaluation of cell-SELEX enriched aptamers binding to breast cancer cells, *Biochimie* 17 (2017). In press.
- [76] T. Sakamoto, E. Ennifar, Y. Nakamura, Thermodynamic study of aptamers binding to their target proteins, *Biochimie* (2017). In press.
- [77] P. Baaske, C.J. Wienken, P. Reineck, S. Duhr, D. Braun, Optical thermophoresis for quantifying the buffer dependence of aptamer binding, *Angew. Chemie – Int. Ed.* 49 (2010) 2238–2241.
- [78] E. Schax, M. Lönne, T. Scheper, S. Belkin, J.G. Walter, Aptamer-based depletion of small molecular contaminants: a case study using ochratoxin A, *Biotechnol. Bioprocess Eng.* 20 (2015) 1016–1025.
- [79] V. Skouridou, M. Jauset-Rubio, P. Ballester, A.S. Bashammakh, M.S. El-Shahawi, A.O. Alyoubi, C.K. O’Sullivan, Selection and characterization of DNA aptamers against the steroid testosterone, *Microchim. Acta.* 6 (2017) 1631–1639.
- [80] Q. Zhu, T. Li, Y. Ma, Z. Wang, J. Huang, R. Liu, Y. Gu, Colorimetric detection of cholic acid based on an aptamer adsorbed gold nanoprobe, *RSC Adv.* 7 (2017) 19250–19256.
- [81] G. Den Van Bogaart, K. Meyenberg, U. Diederichsen, R. Jahn, Phosphatidylinositol 4,5-bisphosphate increases Ca²⁺ affinity of synaptotagmin-1 by 40-fold, *J. Biol. Chem.* 287 (2012) 16447–16453.
- [82] Y. Pang, W. Lan, X. Huang, G. Zuo, H. Liu, J. Zhang, Inhibition of ferric ion to oxalate oxidase shed light on the substrate binding site, *BioMetals* 5 (2015) 861–868.
- [83] M. Asmari, L. Michalcová, H.A. Alhazmi, Z. Glatz, S. El Deeb, Investigation of deferiprone binding to different essential metal ions using microscale thermophoresis and electrospray ionization mass spectrometry, *Microchem. J.* 137 (2018) 98–104.